

Spring 5-2017

# Cost-Effective Monitoring of Railroad Bridge Performance

Jose Alberto Gomez Romero Salazar  
*University of New Mexico*

Follow this and additional works at: [https://digitalrepository.unm.edu/ce\\_etds](https://digitalrepository.unm.edu/ce_etds)



Part of the [Civil and Environmental Engineering Commons](#)

---

## Recommended Citation

Gomez Romero Salazar, Jose Alberto. "Cost-Effective Monitoring of Railroad Bridge Performance." (2017).  
[https://digitalrepository.unm.edu/ce\\_etds/162](https://digitalrepository.unm.edu/ce_etds/162)

This Thesis is brought to you for free and open access by the Engineering ETDs at UNM Digital Repository. It has been accepted for inclusion in Civil Engineering ETDs by an authorized administrator of UNM Digital Repository. For more information, please contact [disc@unm.edu](mailto:disc@unm.edu).

Jose Alberto Gómez Romero-Salazar  
*Candidate*

---

Civil Engineering  
*Department*

---

This thesis is approved, and it is acceptable in quality and form for publication:

*Approved by the Thesis Committee:*

Fernando Moreu, Chair

---

Mahmoud Reda Taha

---

Timothy Jack Ross

---

---

---

---

---

---

---

**COST-EFFECTIVE MONITORING OF RAILROAD BRIDGE  
PERFORMANCE**

**by**

**JOSE ALBERTO GOMEZ ROMERO-SALAZAR**

**B.S., INDUSTRIAL ENGINEERING, CARLOS III  
UNIVERSITY OF MADRID, SPAIN, 2015**

THESIS

Submitted in Partial Fulfillment of the  
Requirements for the Degree of

**Master of Science**

**Civil Engineering**

The University of New Mexico  
Albuquerque, New Mexico

**May, 2017**

## **DEDICATION**

*I dedicate this thesis to everyone that has supported me in this long journey and helped me to overcome it. In particular, I want to thank my parents Paloma and Jose Alberto for teaching me the importance of studying and being patient. To my brother Dieguito and to Nathalia for the unconditional support. Without you it would have not been possible. I love you.*

## **ACKNOWLEDGEMENT**

I want to thank my advisor and committee chair Dr. Fernando Moreu. I also want to thank Dr. Timothy J. Ross and Dr. Mahmoud R. Taha for being in my defense committee. Thank you Dr. Ali I. Ozdagli for devoting infinite hours teaching me how to be a better engineer, a big part of this thesis would not have been possible without you. I also thank Kenny Martinez for helping me with the logistics and experimentation issues in the laboratory. Thank you Serafín García and Abraham Mena for all the support and help.

This research has been funded by the University of New Mexico Teaching Allocation Grant and the Department of Civil Engineering of the University of New Mexico. I would like to acknowledge this funding.

# **COST-EFFECTIVE MONITORING OF RAILROAD BRIDGE PERFORMANCE**

by

Jose Alberto Gómez Romero-Salazar

B.S., Industrial Engineering, Carlos III University of Madrid, Spain, 2015

## **ABSTRACT**

The railroad network carries 40 % of the freight in the US. Railroad bridges are the most critical part of the network and they need to be properly maintained for safety of operations. Railroad managers inspect the bridges to assess their structural condition. Railroad managers are interested in measuring displacements under train crossing events to prioritize their bridge management and safety decisions. However, bridge displacements are difficult to collect in the field, because they require a fixed reference from where to measure. Accelerations can be used to estimate dynamic displacements but to this date, the pseudo-static displacements cannot be measured using reference-free sensors. This study proposes a method to estimate the total displacements of a railroad bridge under live train loads using acceleration and tilt data without a need for fixed reference. Researchers used real bridge displacement data representing different bridge

serviceability level under train traffic. This study explores the design of a new bridge deck-pier experimental model that simulates the vibrations of railroad bridges under traffic. This experiment configuration includes the use of a shake table to input the recorded signal from the field into a railroad pile bent. Reference-free sensors measured both the inclination angle and accelerations of the pile cap. The different acceleration readings are used to estimate the total displacements of the bridge using data filtering. The estimated displacements are then compared to the true responses of the model measured with displacement sensors. The results show that this method can cost-effectively measure the total displacement of railroad bridges without a fixed reference. In addition, this paper studies the use of a low-cost data acquisition platform to measure reference-free dynamic displacements of railroad bridges by combining low-cost microcontrollers and accelerometers. Researchers used the new system to measure accelerations and reconstruct reference-free displacements from several railroad bridge crossing events. The results obtained from the proposed low-cost sensors were compared with those of commercial sensing equipment. The results show that low-cost sensors and commercial sensing systems can measure reference-free displacements with comparable accuracy. The results of this study show that the proposed platform estimates reference-free displacements with a peak error between 20 % and 30 % and a root mean square (RMS) error between 10 % and 20 %, which is similar to commercial SHM systems. The proposed low-cost system is approximately 300 times less expensive than the commercial sensing equipment. In conclusion, this study evaluates the accuracy of cost-effective

systems to measure the reference-free displacement of railroad bridges. The conclusions of this study propose a cost-effective method to measure the reference-free displacement of railroad bridges that all railroad companies can afford. The ultimate goal of this research is to provide stakeholders with means to design, develop, own, and operate their own SHM systems.



# TABLE OF CONTENTS

LIST OF FIGURES.....	X
LIST OF TABLES .....	xiii
Chapter 1 Introduction .....	1
2.2. Railroads in the United States.....	1
1.2 Bridges inside the railroad network .....	2
1.3 Maintenance of railroad bridges.....	4
1.4 Structural health monitoring of railroad bridges: serviceability.....	5
1.5 Outline of thesis .....	7
Chapter 2 Literature review .....	10
2.1 Introduction .....	10
2.2 Performance monitoring of railroad bridges .....	10
2.2.1 Direct displacement estimation .....	11
2.2.2 Displacement estimation from angle of inclination .....	16
2.2.3 FIR filter for dynamic displacement estimation .....	23
2.3 Use of inexpensive sensors for structural health monitoring.....	25
Chapter 3 Inclination angle displacement estimation .....	30
3.1 Introduction .....	30
3.2 Methodology.....	30
3.2.1 Total reference-free displacement .....	30
3.2.2 Moving average filter for pseudo-static displacement estimation.....	31
3.2.3 Performance evaluation criteria .....	33
3.2.4 Procedure overview .....	35
3.3 Experiment .....	37
3.3.1 Railroad bridge testing layout.....	37
3.3.2 Instrumentation .....	38
3.3.3 Railroad bridge displacement data.....	41

3.4 Experimental results.....	41
<b>Chapter 4 Low-cost displacement estimation.....</b>	<b>47</b>
4.1 Introduction .....	47
4.2 Methodology.....	47
4.2.1 Commercial sensing system .....	47
4.2.2 Low-cost sensing system .....	48
4.2.3 Low-cost and commercial sensing systems comparison .....	51
4.2.4 Experiment set-up .....	55
4.2.5 Experimental methodology.....	56
4.2.6 Performance evaluation criteria .....	57
4.3 Experiments and results.....	58
4.3.1 Uniform sinusoidal excitation .....	59
4.3.2 Earthquake displacement estimation .....	64
4.3.3 Train displacement estimation .....	67
<b>Chapter 5 Conclusions and further research.....</b>	<b>71</b>
5.1 Summary .....	71
5.2 Further research.....	73
5.2.1 Wireless implementation .....	73
5.2.2 Power consumption.....	74
5.2.3 Sensor casing and attachment.....	74
5.2.4 Low-cost tilt measurement .....	76
5.4 Limitations .....	78
5.3 Applications.....	78
5.5 Publications related to this MS thesis document.....	79
<b>References .....</b>	<b>81</b>

## LIST OF FIGURES

Fig. 1.1. Freight Railroad Investment since 1980 (AAR 2015). .....	2
Fig. 1.2. Railroad network capacity evolution prediction (Cambridge Systematics, 2007). .....	3
Fig. 1.3. Railroad bridge visual inspection. ....	4
Fig. 1.4. Railroad bridge under service load. ....	7
Fig. 2.1. Crane-aided visual inspection of railroad bridge (N.E. Bridge Contractors 2016). .....	11
Fig. 2.2. Scaffolding to provide fixed reference point for displacement measurement of a railroad bridge (Moreu et al. 2015). ....	12
Fig. 2.3. Measurement of the deflection of a railroad bridge using a RTS (Psimoulis and Stiros, 2013). ....	13
Fig. 2.4. Measurement of a railroad bridge vibration using a LDV (Nassif et al. 2005). ....	15
Fig. 2.5. Sensor configuration for railroad bridge displacement estimation (Hoag et al. 2017). ....	16
Fig. 2.6. Instrumentation detail showing accelerometers and LVDTs for reference-free displacement estimation (Moreu et al. 2015). ....	18
Fig. 2.7. Inclinator position illustration (Hou et al. 2005). ....	19
Fig. 2.8. Shake table and controller box on the Smart Management of Infrastructure Laboratory (SMILab 2017). ....	21
Fig. 2.9. Schematic representation of displacement components of railroad bridge. ....	22

Fig. 2.10. Graphical representation of displacement estimation from acceleration performance between double integration and FIR filter. ....	25
Fig. 2.11. Test set-up for reference-free displacement measurement with a smartphone (Min et al. 2016). ....	27
Fig. 2.12. Arduino UNO board (Embedded Computing Design 2016). ....	27
Fig. 3.1. Schematic relation between tilt and displacement of a railroad timber trestle. ....	31
Fig. 3.2. Graphical demonstration of designed filter. ....	33
Fig. 3.3. Methodology of the tilt angle estimation from displacements. ....	36
Fig. 3.4. Final set-up for railroad bridge tilt measurement. ....	38
Fig. 3.5. 3711B110G accelerometers close-up. ....	39
Fig. 3.6. Vibpilot Data Acquisition System. ....	40
Fig. 3.7. Final set-up for railroad bridge tilt measurement. ....	40
Fig. 3.8. Bridge displacement estimation under NB 3.1 km/h train. ....	42
Fig. 3.9. Pseudo-static displacement estimation. ....	43
Fig. 3.10. Dynamic displacement estimation. ....	44
Fig. 3.11. Total displacement estimation. ....	44
Fig. 3.12. Error values of the total displacement estimation. ....	45
Fig. 4.1. 353B33 ICP accelerometer close-up. ....	48
Fig. 4.2. Low-cost accelerometers (a) ADXL345, (b) ADXL362, (c) MMA8452Q. ....	50
Fig. 4.3. Arduino UNO and ADXL345 accelerometer. ....	51

Fig. 4.4. Quantization errors of the used accelerometers. ....	52
Fig. 4.5. Displacement estimation experimental set-up (plan view from above). ....	55
Fig. 4.6. Experimentation methodology flow chart. ....	56
Fig. 4.7. Displacement estimation comparison for MMA8452Q and Capacitive to LVDT. ....	60
Fig. 4.8. Error values for ADXL345 vs ICP for sine wave tests. ....	61
Fig. 4.9. Error values for ADXL362 vs ICP for sine wave tests. ....	61
Fig. 4.10. Error values for MMA8452Q vs Cap for sine wave tests. ....	62
Fig. 4.11. Comparison of errors of the displacement estimations. ....	63
Fig. 4.12. El Centro earthquake displacement estimation. ....	65
Fig. 4.13. Error values for Capacitive vs ADXL362 vs MMA8452Q for earthquake tests. ....	65
Fig. 4.14. Train displacement estimation for the 41 km/h NB case. ....	68
Fig. 4.15. Error values for Capacitive vs ADXL362 vs MMA8452Q for train tests. ....	68
Fig. 5.1. Low-cost wireless connection configuration. ....	74
Fig. 5.2. Schematic configuration of final sensor. ....	75
Fig. 5.3. Low-cost tilt measurement estimation set-up. ....	77

## LIST OF TABLES

Table 1.1. Ranking of 2010 railroad bridge research topics (Moreu et al. 2012). .....	5
Table 3.1. Train characteristics description. ....	41
Table 3.2. Total displacement estimation errors. ....	46
Table 4.1. Sensor cost comparison. ....	54
Table 4.2. Description of sinusoidal wave excitation characteristics. ....	59
Table 4.3. Uniform sinusoidal excitation errors. ....	63
Table 4.4. Earthquake displacement estimation error. ....	66
Table 4.5. Train characteristics description. ....	67
Table 4.6. Train displacement estimation error. ....	69

# **Chapter 1 Introduction**

This research explores and quantifies cost-effective monitoring systems to assess the serviceability of railroad bridges. The results of this work are (1) a new method to estimate the pseudo-static component of the displacement of the railroad bridge and (2) the quantification of the quality of low-cost sensing to measure reference-free dynamic displacements of bridges under train traffic. This research focuses on using acceleration data obtained from the vibration of the railroad bridge to estimate the displacement. The first method is based on the application of trigonometric relations to obtain the angle of inclination of the bridge pier and calculate the estimated pseudo-static displacement from it. The second method of low-cost sensing consists on attaching a low-cost accelerometer to the deck of the bridge model and collecting the acceleration data when the train is passing by. After the data is collected, it is transformed into displacement using a finite impulse response filter and then compared to commercially available sensors. The following sections in this chapter motivate the importance of cost-effective serviceability monitoring objective quantification in the context of railroad bridge management.

## **2.2. Railroads in the United States**

The North American railroad network is considered the best freight system in the world (GeoMetrx, 2013). Railroads perform 40 % of the US freight transportation in terms of ton-miles (Federal Railroad Administration (FRA), 2010). The demand for the railroads is increasing every year, and to meet this interest,

the investment has been increasing steadily. Fig. 1.1 shows the investment increase on the railroad network since 1980, and, according to the association of American railroads (AAR), the U.S. Federal Highway Administration estimates that total U.S. freight shipments will increase 45 percent by 2040 (AAR 2015).

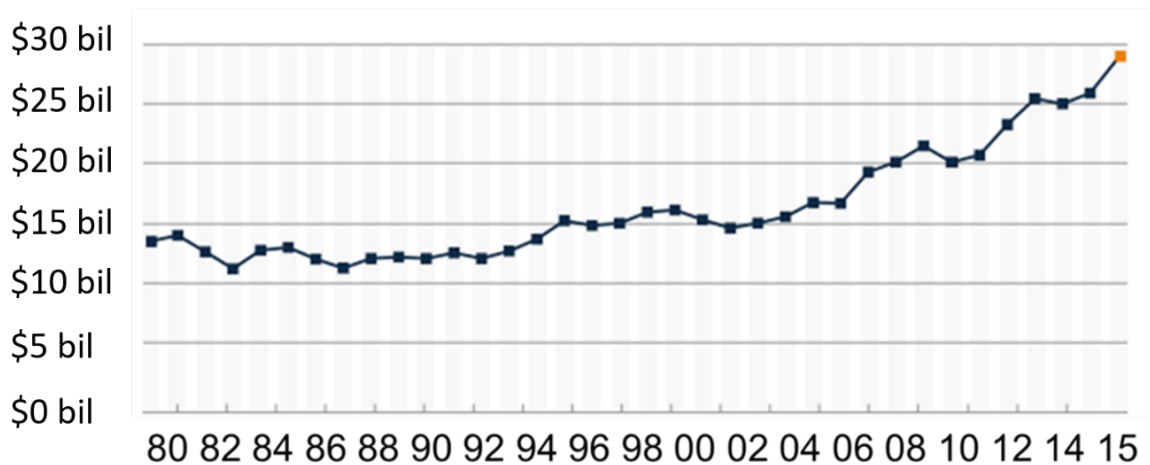


Fig. 1.1. Freight Railroad Investment since 1980 (AAR 2015).

In 2014, a study conducted by Towson University pointed out that the economic activity of Class I railroads was almost \$274 billion (AAR 2016). The railroad network is aging and the weight of the cars have augmented throughout the years (Unsworth 2010). Fig. 1.2 illustrates the projected railroad network capacity from 2007 to 2035 (Cambridge systematics 2007). The prediction states that the majority of the railroad network will be at its capacity or above it by 2035.

## 1.2 Bridges inside the railroad network

There are approximately 100,000 railroad bridges in the United States, nearly one for every 1.4 miles of track. Today, more than half of US railroad bridges



are over one hundred years old (AREMA 2003), which makes bridge management and maintenance a top priority for the safety of freight rail industry (Moreu, 2015).

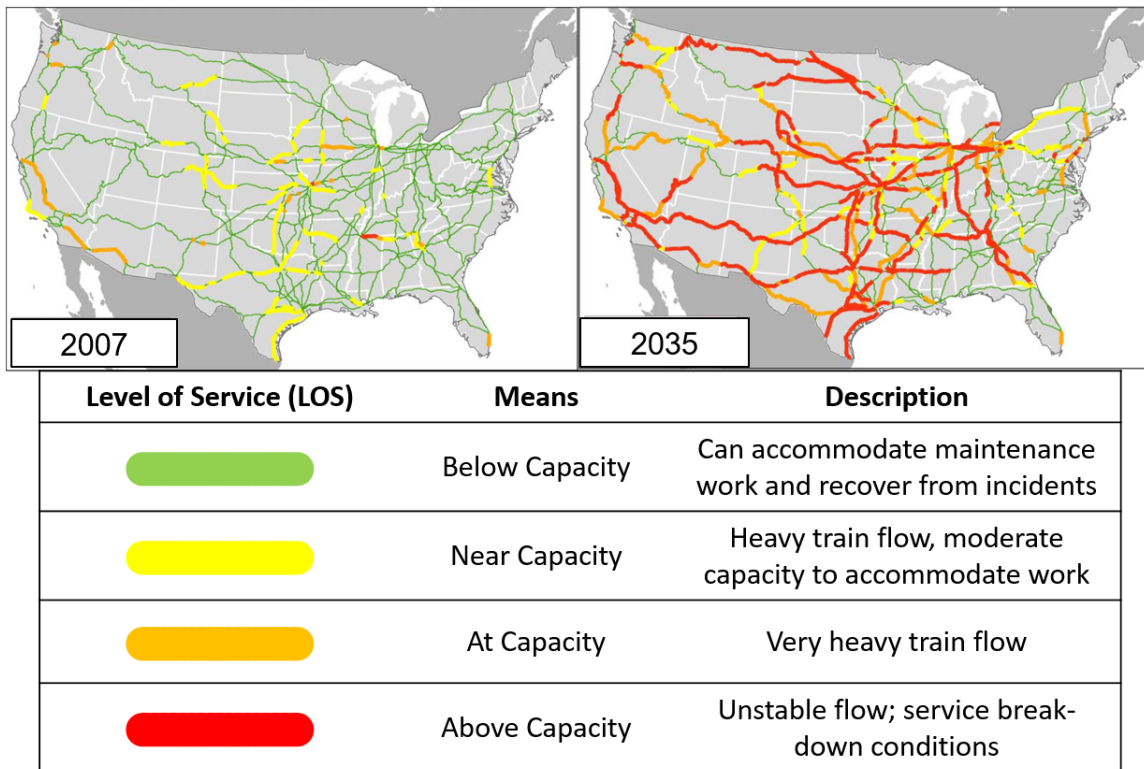


Fig. 1.2. Railroad network capacity evolution prediction (Cambridge Systematics, 2007).

According to the FRA the traffic density and loads are increasing year after year and the consequences of a bridge failure would be catastrophic (FRA 2010), which remarks the crucial importance of railroad bridge maintenance. In 2013, approximately the 34 percent of the money invested on railroads (around 22 Billion dollars) was spent on the maintenance and modernization of it (AAR 2013). In 2011, railroads invested \$600 million in bridge maintenance to ensure freight is safely and efficiently transported across the country (AAR 2013).

### 1.3 Maintenance of railroad bridges

Maintenance, repair, and replacement (MRR) strategies of railroad bridges are necessary to allocate funds where they are most needed. Because of the fund limitations and demand growth, it is necessary to develop cost-effective strategies to manage the railroad bridge network (Moreu and LaFave 2012). Bridges are inspected to ensure their structural condition to safely carry trains. However, current inspections are conducted mostly visually and without trains crossing the bridge due to limited access and safety (AAR 2016). Fig. 1.3 shows a railroad bridge visual inspection.



Fig. 1.3. Railroad bridge visual inspection.

Agdas et al. (2015) stated that visual inspections of bridges do not provide reliable information and suggested using data-driven strategies. Moreover, a survey conducted in 2010 among railroad bridge structural engineers revealed that

their main research interest was to obtain the displacement of the bridge during the train crossing event (Moreu et al. 2012). Table 1.1 illustrates the major 2010 railroad bridge research topics addressed by Moreu and LaFave (2012), where it can be observed that the first concern was to measure the deflection of the bridge under live loading.

Table 1.1. Ranking of 2010 railroad bridge research topics (Moreu et al. 2012).

2010 Topics	2010 Ranking
Deflection Measurements	1
High speed trains	2
Long-span bridges	3
Approaches	4
Longitudinal forces	5
New design loads	6

#### **1.4 Structural health monitoring of railroad bridges: serviceability**

Structural health monitoring (SHM) is a solution that researchers want to implement to assess the structural condition of bridges. In effect, SHM seeks to provide accurate information about the status of the structure avoiding catastrophic failures (Balageas 2006). In the case of bridges, there is the possibility that damage could go undetected due to the nature of the inspections or that the existing damage could reach critical levels between inspections. Multiple

researchers have been studying different techniques of damage detection of bridges (Farrar et al. 1994, Zhang and Aktan 1995, Villemure et al. 1996, Nickitopoulou et al. 2006 and Moreu et al. 2015). The FRA sponsored a study to investigate possibilities and options to implement SHM of railroad bridges in the US in 1994. The results from this study revealed that the cost estimation of installing sensors on the entire railroad bridge network amounted to several billions of dollars, with an extra 60 million a year for maintenance (Perez-Pena, 1996). Researchers have explored railroad bridge structural health monitoring for long-term efforts. However, the currently proposed instrumentation is expensive and difficult to implement. In addition, the portability and availability of this instrumentation for railroad environment is limited due to the tight traffic schedules and access to the structure (Fig. 1.4). Therefore, even when railroad managers are exploring new technologies to assist them to quantify the performance of their railroad bridges in their day to day operations, the complexity and cost of the existing technologies and the amount of data prevents them from implementing them. If a simple, effective, low-cost monitoring technique would be proposed, validated, and tested, railroad managers would consider their adoption for bridge serviceability assessment. In conclusion, the cost and complexity of the existing technologies prevents them to be implemented in day-to-day operations in railroad bridges.



Fig. 1.4. Railroad bridge under service load.

## 1.5 Outline of thesis

This research proposes a method to estimate the total displacements of a railroad bridge under live train loads without a need for fixed reference for performance assessment under trains. Researchers used real bridge displacement data representing different bridge serviceability level under train traffic. This study explores the design of a new bridge deck-pier experimental model that simulates the vibrations of railroad bridges under traffic. The different acceleration readings are used to estimate the total displacements of the bridge using data filtering. The estimated displacements are then compared to the true responses of the model measured with displacement sensors. The results show that this method can cost-effectively measure the total displacement of railroad bridges without a fixed reference. In addition, this paper studies the use of a low-cost data acquisition platform to measure reference-free dynamic displacements

of railroad bridges by combining low-cost microcontrollers and accelerometers. The results obtained from the proposed low-cost sensors were compared with those of commercial sensing equipment. The results show that low-cost sensors and commercial sensing systems can measure reference-free displacements with comparable accuracy. The final objective of this research is to provide railroad managers with a reliable and affordable method to assess the structural status of the railroad bridges.

A short description of each of the chapters of this research is provided below:

Chapter 2 of this thesis explores the literature related to the topic and covers the recent investigations conducted on the fields of railroad bridge monitoring and railroad bridge safety as well as the investigations on the use of the angle of inclination of the structure to determine its structural health. It also reviews the use of inexpensive sensors for structural health monitoring. The information collected from this chapter will put the contributions of this thesis in its context.

Chapter 3 defines the estimation of the total displacements of the railroad bridge deck based on the angle of inclination of the bridge pier. The materials used, the set-up configuration and the data processing procedures are also described in this chapter. In the last part of the chapter, the results are discussed.

Chapter 4 describes the bridge dynamic displacement estimation method using low-cost sensors. It includes the description of the materials used, the test procedures and their evolution to simulate the train conditions as accurately as

possible. This test also includes the set-ups used and the description of the used data analysis techniques. Finally, the results obtained are displayed and analyzed.

Chapter 5 draws the conclusions obtained from both types of displacement estimations and gives some recommendations for future research steps.

## **Chapter 2 Literature review**

### **2.1 Introduction**

In this chapter, background information of the current methods and on-going research projects that are being conducted related to structural health monitoring of railroad bridges is described. The first part of the chapter consists on an outline of the importance of measuring the displacements of the railroad bridge deck. Then, the chapter continues by describing some of the techniques that are currently used to measure those displacements. The second part defines some of the current low-sensing methods used for structural health monitoring. Finally the chapter ends with a description of the new contributions that this thesis provides.

### **2.2 Performance monitoring of railroad bridges**

Currently, railroad bridge inspections mainly consist of visual evaluation of the bridge status. Fig. 2.1 shows a railroad bridge inspection. These inspections need to be conducted without trains on the bridge, and hence cannot live load behavior on their evaluations, which might result in unseen defects or unusual bridge responses.

Measuring the bridge displacements can help to assess its structural health and notify of an anomalous situation. The bridge displacements relate directly to the structural condition of the bridge and can be used to determine different bridges serviceability (Moreu et al. 2015). A good understanding of the nature of the displacements that occur on a railroad bridge can help assessing its structural performance.





Fig. 2.1. Crane-aided visual inspection of railroad bridge (N.E. Bridge Contractors 2016).

### 2.2.1 Direct displacement estimation

Displacement sensors such as linear variable differential transducers (LVDTs) can measure displacements by placing them in the direction of motion and providing a fixed reference point. Moreu et al. (2014) collected the railroad bridge transverse displacements using LVDTs under different traffic conditions to investigate the effect of different speeds and loads on the bridge behavior. Uppal et al. (1990) also used LVDTs to measure the displacements of timber railroad bridges to prove that different train speeds influence the deflections of the bridge deck. Sundaram et al. (2015) used LVDTs among other sensors to measure the displacements of a prestressed concrete slab bridge and monitor the responses under heavy axle freight wagons. The purpose of this research was to study the

effect of the higher tractive / braking forces on the bridge. Likewise, Fanning et al. (2005) and Nassif et al. (2005) used LVDTs for direct displacement measurement.

Fig. 2.2 illustrates the difficulties of providing a fixed reference point for direct displacement measurement of railroad bridges. In the case of the figure, a ten-thousand-dollar scaffold was built to provide the mentioned fixed reference point with the ground.



Fig. 2.2. Scaffolding to provide fixed reference point for displacement measurement of a railroad bridge (Moreu et al. 2015).

Traditional methods to measure displacements under live load require a fixed reference point, which is expensive to provide and sometimes not even possible. Due to the challenges and difficulties for bridge displacement measurement, researchers have studied contact-free and reference-free displacement measurement methods. Psimoulis and Stiros (2013) proposed the use of a robotic total station (RTS) to measure the deflections of a short-span

railroad bridge in response to passing trains. A RTS is equipped with an automatic target recognition device, which allows locking onto a target and measuring its coordinate changes with respect to the initial position of the bridge. This device requires advanced algorithms to record the changes of the bridge displacement. However, the accuracy of this method depends on specific atmospheric conditions. Additionally, the necessary equipment is expensive, and it is not suitable for long term monitoring. Fig. 2.3 shows the set-up used by Psimoulis and Stiros to measure the deflections of a real bridge with a RTS.



Fig. 2.3. Measurement of the deflection of a railroad bridge using a RTS (Psimoulis and Stiros, 2013).

Several researchers (Murray 2013, Hoag 2017) investigated digital image correlation (DIC) techniques to quantify the displacements of a railroad bridge. DIC is a method used to calculate displacements based on the changes in the texture (i.e. color) of digital images with respect to an initial reference image. Some of the most important drawbacks are the dependency on the image quality, atmospheric

conditions, and noise. If it was necessary to monitor a large number of locations on the bridge, this method requires an expensive setup consisting multiple high-quality cameras for increased resolution. Nickitopoulou et al. (2006) proposed the monitoring of deformations of large slender structures with Global Positioning System (GPS) and proved the level of accuracy of the method estimating the displacement of a rotating body with constant angular velocity and compared the estimations with the known displacement data. The results obtained showed a 1.5 % of error for displacements larger than 15 mm. Watson et al. (2007) used GPS to monitor the deflections of a cable-stayed bridge and compare the results with the predictions of a computer model. Their results demonstrated a displacement accuracy with a resolution of 3.5 mm. The downsides of these methods are the high implementation cost and the insufficient accuracy for small vibration applications, which makes them unsuitable for the majority of railroad bridge monitoring applications. Nassif et al. (2005) utilized a Laser Doppler Vibrometer (LDV) to measure the deflection and vibration of bridges. The LDV measures the velocity and displacement of the vibrating object by detecting the frequency shift of the reflected light. Nevertheless, this method has two major drawbacks. The first one is the high cost of the LDV and the second one is that the device is not suitable for long-term monitoring due to the inability of leaving it unattended. Fig. 2.4 shows the configuration employed by Nassif et al. to measure the vibrations of the bridge deck with a LDV.



Fig. 2.4. Measurement of a railroad bridge vibration using a LDV (Nassif et al. 2005).

Yang et al. (2005) developed a simple approach to obtain the displacements of structures under earthquake motions from the measured accelerations. Their objective was to avoid the errors resulting from simple double integration of the acceleration. The authors indicated the feasibility and effectiveness of the method proposed validating it with numerical examples. Gindy et al. (2008) employed a state-space approach to obtain the displacements of a bridge from the measured accelerations. They validated this method in the field by comparing the estimations to displacement sensor responses. The major drawback of these methods is that they require information about initial conditions, which is in general not known in real life applications. Moreu et al. (2015) proposed an alternative method to estimate railroad bridge reference-free displacements by measuring the accelerations using a finite impulse response (FIR) filter that can accurately estimate dynamic displacements. They validated their method by placing wireless

smart sensors (WSS) on a timber railroad bridge and estimating their displacements.

### 2.2.2 Displacement estimation from angle of inclination

A common problem of the mentioned studies is that they require a fixed reference from where to measure the responses with respect to that position (even when using lasers or DIC). However, providing a reference is sometimes difficult, especially when bridges are spanning over big geographical obstacles such as rivers, lakes or gaps between mountains. Fig. 2.5 shows the used set-up on the bridge to capture the displacements of a bridge under trains.

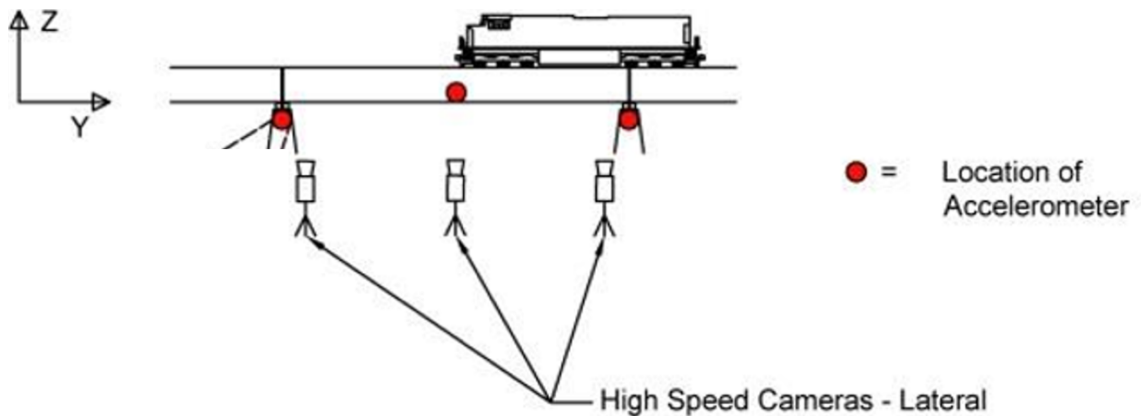


Fig. 2.5. Sensor configuration for railroad bridge displacement estimation (Hoag et al. 2017).

Researchers have explored the acceleration measurements to estimate reference-free displacements. Traditional methods usually double integrated the acceleration readings to obtain the displacements and filtered to remove the

integration errors. Boore (2003), Yang et al. (2005) and Gindy et al. (2008) are among the researchers that have explored the possibility of estimating the displacements from the acceleration. Besides the SHM applications, this problem is frequently encountered in inertial navigation systems (INS) applications. The use of accelerometers to estimate displacements or positions is frequently used when other positioning technologies such as GPS are not available or are not advisable (Ojeda and Borenstein, 2007). These researchers implemented an inertial measurement unit (IMU) system designed for subject tracking. An IMU is a sensing system that consists of a three-degree-of-freedom accelerometer and a three-degree-of-freedom gyroscope. They used quaternion-type vectors to define the attitude of the sensor and implemented an optimized discrete time algorithm to reduce the errors from the sensors. Other INS researchers have used a Kalman filter as the error reduction technique to estimate the position or displacement from the acceleration values (Roumeliotis et al., 2002; Sabatini, 2006). Park et al. (2013) used a finite impulse response (FIR) filter to estimate zero-mean displacements from accelerations. They used accelerometers to capture the motion inputted by a shake table. Moreu et al. (2015) used a similar approach to estimate the displacements of a real railroad bridge using wireless smart sensors (WSS) and comparing the estimations to LVDT readings. Fig. 2.6 shows the sensing systems used by Moreu et al. (2015) to obtain reference-free displacement measurements of a railroad bridge.

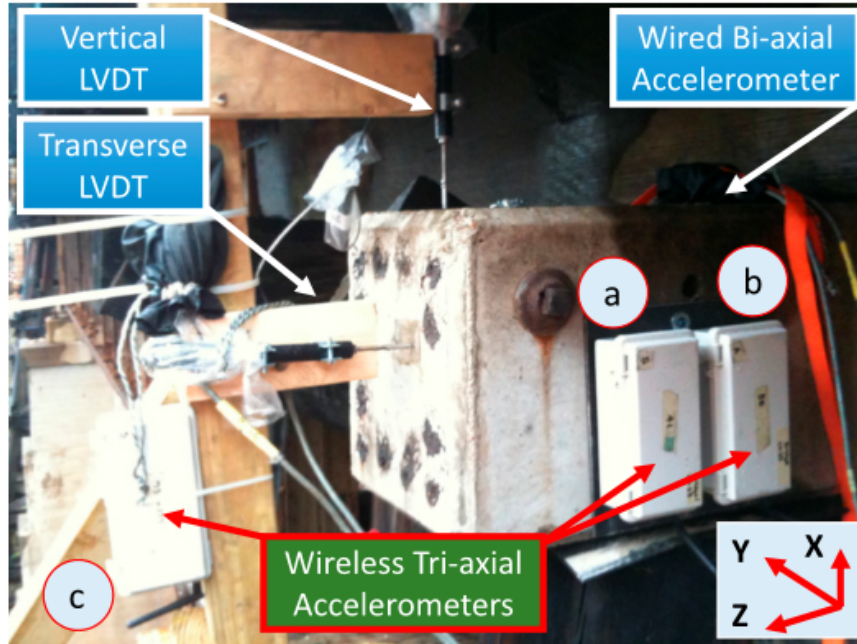


Fig. 2.6. Instrumentation detail showing accelerometers and LVDTs for reference-free displacement estimation (Moreu et al. 2015).

However, these methods cannot be directly applied to railroad bridges due to the nature of the bridge displacement. There are two observable components in the displacement of a railroad bridge, the high frequency dynamic displacement due to the vibrations of the bridge during the train crossing and the low frequency pseudo-static component due to the weight of the train (Stephen et al. 1993). The dynamic component is a zero-mean displacement that is produced by the impact of the train with the track. The pseudo-static component can be described as the displacement that would be observed on the bridge if the train was not moving. Accelerometers are inertial sensors and can only measure dynamic excitations due to their zero-mean nature. Hoag et al. (2017) conducted experiments to obtain and compare the displacements of a railroad bridge using digital image correlation



(DIC) and accelerometers. The results of their research concluded that the pseudo-static component of the railroad bridge displacement cannot be measured with reference-free sensors. Consequently, it is possible to measure dynamic non-contact, reference-free displacements, but it is not possible to cost-effectively obtain the pseudo-static component of displacements during field monitoring campaigns using current methodologies.

Researchers have developed alternative reference-free methods for measuring the displacements of bridges to avoid the need for a fixed reference. One of the most commonly utilized methods consists of measuring the inclination of the bridge deck to obtain the displacements. Hou et al. (2005) defined a method for calculating the vertical deflection by attaching several inclinometers along the span of a bridge and computed its angle of inclination over time. Then, they calculated the deflection of the span by differentiating the angular values and obtained the deflection curve. The minimum number of inclinometers needed in order for the method to work is five. The precision of the method increases when more sensors are used. Fig. 2.7 illustrates the position of the inclinometers used by Hou et al. (2005) to estimate the bridge deflection.

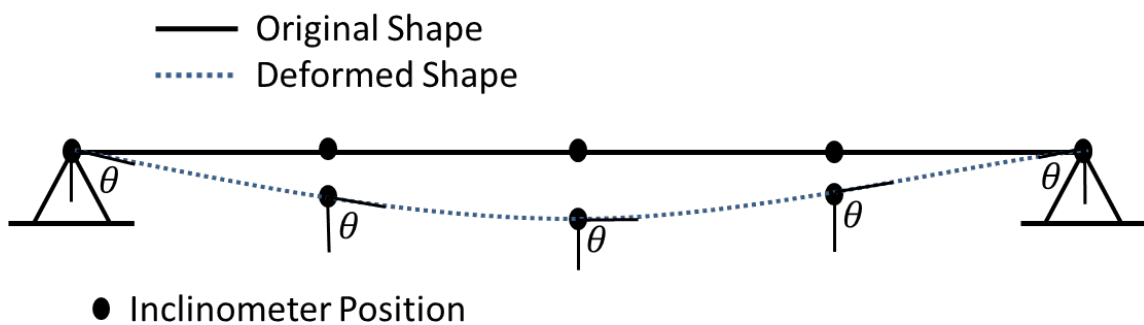


Fig. 2.7. Inclinometer position illustration (Hou et al. 2005).

Yu et al. (2013) used inclination sensors to calculate the deflection of bridges to assess their structural health. However, the authors simplified their method to a centered point load and a uniform distributed load, hence calculating the mid-span point only. Zhang et al. (2016) presented a deflection and damage estimation method based on the relation between the forces and inclinations present in the bridge. They built a finite element model (FEM) of the bridge and combined it with the measured inclinations. The deflections were then reconstructed from the inclinations and the changes in the nodal loads were used as damage indicators. All these researchers proposed methods to estimate the deflection of the bridge. However, those methods are based on complex computer models of the bridges, cannot be used for field monitoring of multiple bridges, and are focused only in the vertical displacements of the bridge, not accounting for the transverse behavior of the bridge under the service loads.

This research proposes a new method to measure the total transverse displacements of railroad bridges under train traffic that is cost-effective, portable, and can be used for simplified serviceability monitoring of bridges networks. To validate this method, this research used real bridge displacement records and experimental models of timber railroad bridges in North America in coordination with one Class I railroad. This new method combines both the pseudo-static and the dynamic components of the railroad bridge displacement. The pseudo-static component of the bridge displacement is attributed to the angle of inclination of the pile bent. In this method, the angle of inclination of the pile bent is obtained by measuring the time history of the gravity components and relating them

trigonometrically. Following assumptions indicated by railroad bridge experts, the relation between the angle of inclination of the pile bent and the displacement is assumed linear. Researchers built a representative pile bent model on a shake table to run the train crossing simulations and validate the method under real railroad bridge displacement data collected in the field. A shake table is a laboratory instrument originally design to test structure models under earthquake simulations (Quanser 2016). However, due to the nature of the bridge vibrations produced by the train, this paper utilized the shake table as the bridge vibration under the train. The instrumentation consists on (1) the table, which reproduces the inputted vibrations and (2) a controller box that provides the connection between the computer and the table. Fig. 2.8 shows a picture of the shake table and the controller box.

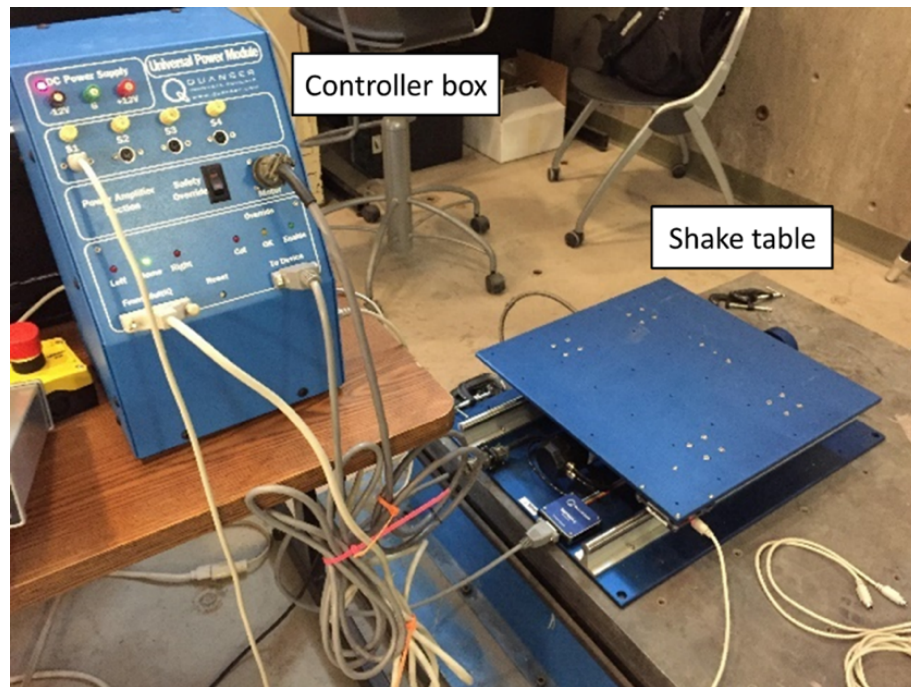


Fig. 2.8. Shake table and controller box on the Smart Management of Infrastructure Laboratory (SMILab 2017).

An LVDT measured the displacement of the shake table was measured to evaluate the accuracy of the system. Two accelerometers placed on the pier of the model measuring responses in the vertical and horizontal directions captured the angular data. A filter extracted the trend from the angle measurements taken from the pile bent of the model. Then, researchers transformed the angular data into displacement using a linear trigonometric relationship. In addition, another accelerometer was placed in the direction of motion of the shake table to capture the dynamic component of the displacement by applying a finite impulse response (FIR) filter to the acceleration data. Finally, researchers combined both components of the displacement (dynamic and pseudo-static) to obtain the total displacement estimation. Ten real bridge displacements were used to validate the method.

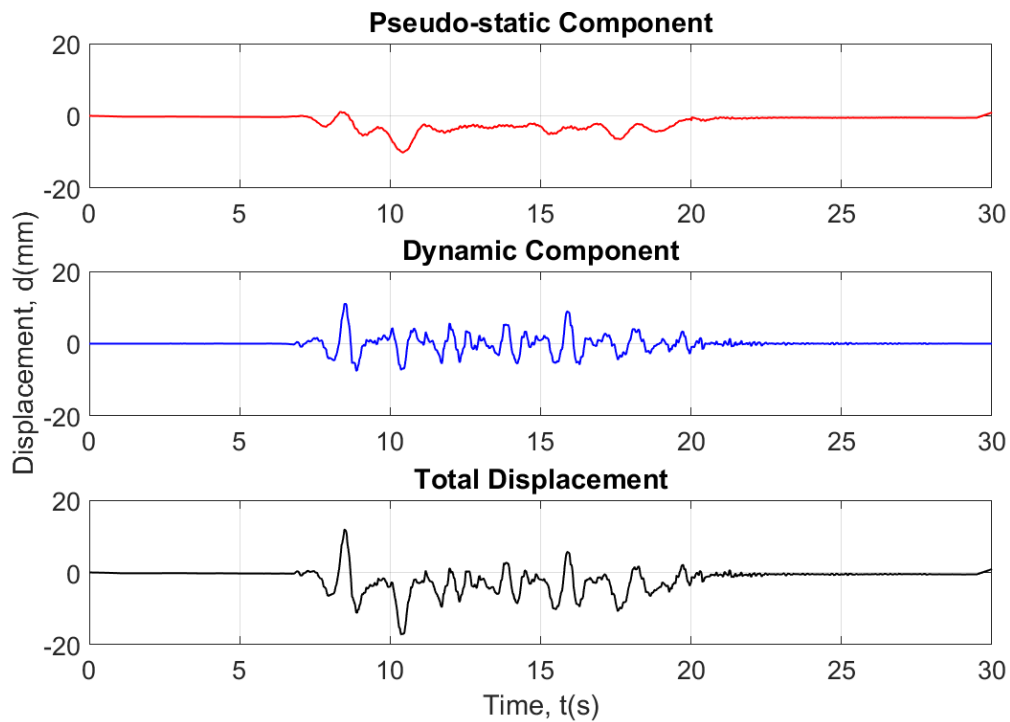


Fig. 2.9. Schematic representation of displacement components of railroad bridge.

The errors between the total displacement estimation and the reference displacement were less than 15 %, demonstrating the accuracy of the method and its ability to obtain the total reference-free displacement of a railroad bridge under trains. Fig. 2.9 shows the total displacement of a railroad bridge deck with its two differentiable components.

### 2.2.3 FIR filter for dynamic displacement estimation

Lee et al. (2010) developed a finite impulse response (FIR) filter to reconstruct displacements from accelerations. This algorithm allows the researchers to reduce the errors produced by the traditional double integration method. The problem is defined by introducing the minimization problem shown in equation 2.1.

$$\min_u \Pi_E(u) = \frac{1}{2} \int_{T_1}^{T_2} (a(u(t)) - \bar{a})^2 dt \quad (2.1)$$

where  $u$  is the displacement that is being calculated,  $a$  is the theoretical acceleration for the double integration method and  $\bar{a}$  is the measured acceleration.

The acceleration is then discretized using the finite differences approximation method and the discretized acceleration is introduced in the minimization problem in equation 2.1. To avoid having an ill-posed problem, a Tikhonov regularization is performed with the addition of a regularization factor  $\lambda$  as shown in equation 2.2.

$$\text{Min}_u \Pi(u) = \frac{1}{2} \|Lu - (\Delta t)^2 L_a \bar{a}\|_2^2 + \frac{\lambda^2}{2} \|u\|_2^2 \quad (2.2)$$

where  $L_a$  is a diagonal matrix with all the diagonal elements equal to one with the exception of the first and the last elements which are equal to  $\frac{1}{\sqrt{2}}$ ,  $L$  is the diagonal weighing matrix product of  $L_a$  and  $L_c$  (linear algebraic operator from finite differences method),  $u$  is the estimated displacement,  $\Delta t$  is the time increment,  $\bar{a}$  is the measured acceleration and  $\lambda$  is the optimal regularization factor.

Equation 2.3 gives the solution with respect to the unknown displacement  $u$ :

$$u = (L^T L + \lambda^2 I)^{-1} \cdot L^T L_a \bar{a} (\Delta t)^2 = C \bar{a} (\Delta t)^2 \quad (2.3)$$

where  $I$  is the identity matrix and  $C$  is the coefficient matrix required for the displacement reconstruction. Multiple researchers have validated this algorithm for different applications (Park et al. 2013; Moreu et al. 2015). In fig. 2.10 a graphical representation of the displacement estimation using traditional double integration and the described FIR filter is shown. In the figure, a sinusoidal wave acts as the reference displacement and the blue and the black curves are displacement estimations from the accelerations taken during the same event. The figure shows how the double integration curve differs with the reference displacement one due to the unknown integration constants. On the other hand, the FIR estimation coincides accurately with the reference displacement. This research uses this algorithm to estimate the dynamic displacement component of the railroad bridge under real train traffic using reference-free sensors.

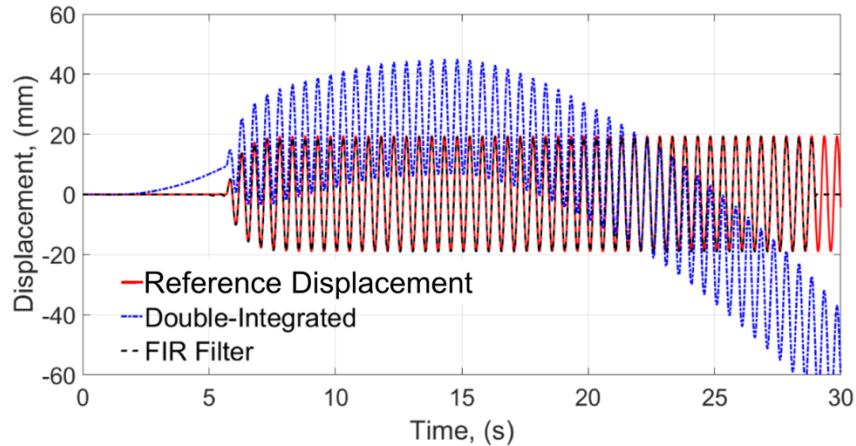


Fig. 2.10. Graphical representation of displacement estimation from acceleration performance between double integration and FIR filter.

### 2.3 Use of inexpensive sensors for structural health monitoring

Commercial WSS systems are expensive and in general complex to be operated by railroad personnel. One of the most common limitations of commercial methods is that railroads need to pay a high cost to consultants and contractors to operate them for data collection, and the data is difficult to access by the owner. The data acquisition for long term applications increases the cost and limits the interest of railroad owners. The implementation of monitoring could become accessible and affordable to all railroads if the sensing monitoring was simplified and the costs lowered.

Researchers have studied low-cost data acquisition platform alternatives for various SHM applications to provide owners with affordable monitoring of structures. For example, Kim et al. (2007) deployed low-cost sensors on the Golden Gate Bridge in San Francisco, CA to record the vibration data of the longest span to find its fundamental modes and compared it with the previous existing models and past studies. The developed sensor network provided reliable and

calibrated data for analysis. Peairs et al. (2004) proposed an accessibility improvement for impedance-based SHM, which consists of utilization of high-frequency structural excitations (typically above 30 kHz) through a surface-bonded piezoelectric sensor/actuator to detect changes in structural response. These researchers showed that the inexpensive impedance sensor responses were as effective as the traditional impedance sensors. Yu et al. (2012) implemented smartphones as SHM sensors and data acquisition systems. They used a smartphone and a wireless inclinometer to record the swing motion of a pendulum model. Min et al. (2016) developed a smartphone application to measure dynamic displacements and process them in real time. The system allows up to 240 frames per second for displacement calculation and real-time display. The authors validated that method by comparing its performance with commercial displacement sensors. However, smartphone measurements require proximity of the inspector to the structure during the measurement. Fig. 2.11 shows the used set-up by Min et al. (2016) to capture reference-free displacements with a smartphone.

Chougule et al. (2010) proposed the implementation of low-cost wireless sensors to ensure the long life operation of wind turbines. These researchers introduced the use of Arduino (Arduino 2015) microcontrollers to make the measurements. Arduino microcontrollers are easy to acquire and to use. They are used for simple projects such as lighting lamps or for complicated and specific research applications.



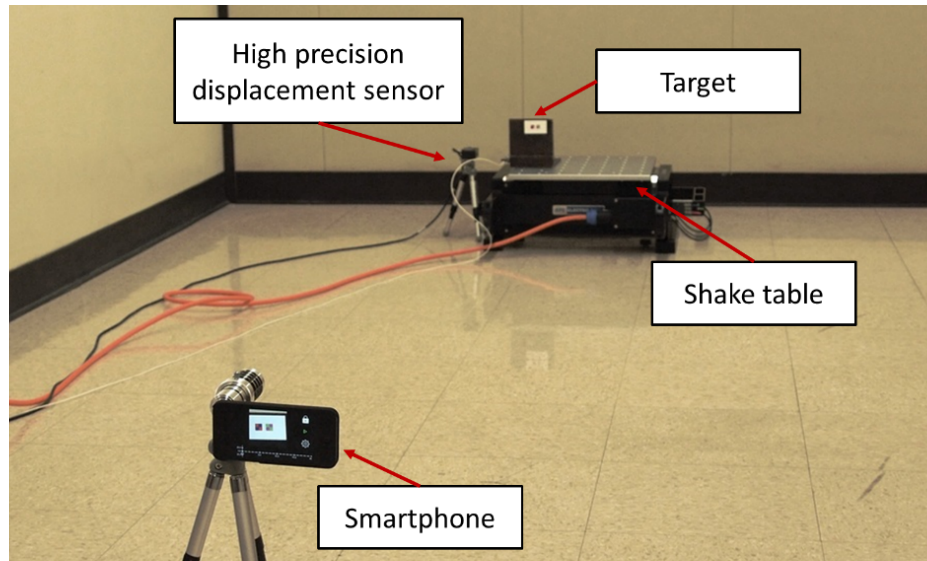


Fig. 2.11. Test set-up for reference-free displacement measurement with a smartphone (Min et al. 2016).

These researchers used it to investigate the suitability of these devices for SHM. Andò et al. (2014) utilized Arduino to propose a multi-sensor system to detect accelerations and inclinations of buildings and structures. They conducted preliminary tests to validate the method and concluded that the use of Arduino for SHM can be a breakthrough for the industry. Fig. 2.12 shows the Arduino UNO board.

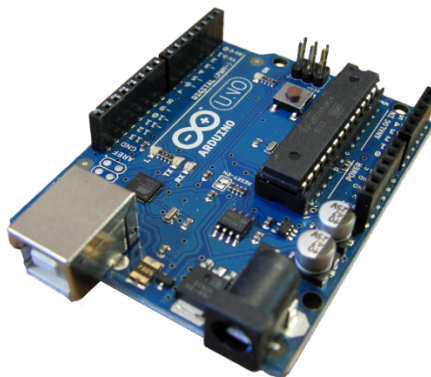


Fig. 2.12. Arduino UNO board (Embedded Computing Design 2016).

The goal of these researchers was to make SHM more accessible to the common public and companies by reducing the cost of sensing devices and data acquisition systems. However, current efforts lack an implementation of low-cost sensors to remotely measure reference-free displacements of bridge responses under real train crossing events.

This research studies using low-cost sensors to measure reference-free transverse displacement of railroad bridges under traffic that can cost-effectively inform railroad owners of bridge safety and performance. This study proposes a sensing system that is affordable both in cost and simplicity and that infrastructure owners can acquire, develop, and use directly. In this study, researchers tested an Arduino microcontroller with low-cost accelerometers to measure the reference-free displacements of multiple railroad bridge train crossing events. The previously mentioned shake table generated the excitations and the accelerations were recorded with both low-cost and commercial sensors. The researchers reconstructed the displacements from the accelerations using a FIR filter. The experiments consisted of multiple sets of signals used to compare the different systems. The displacement of the shake table set the reference for the comparison with the estimated displacements. Then, the errors between the estimations and the reference displacement were calculated to assess the accuracy of the sensors. The error values obtained with the low-cost sensors are equivalent to the ones of the commercial accelerometer. The cost difference with the respect to the commercial accelerometers is of about 300 times. The peak error percentages are between 20 % and 30 % while the RMS error values are between 10 % and 20 %.

The findings of this study indicate that low-cost sensors have the potential to become a cost-effective alternative to monitor railroad bridges responses under traffic. Railroad companies can buy, develop and implement the proposed low-cost system in-house, and obtain similar cost-efficacy for bridge performance monitoring.

## **Chapter 3 Inclination angle displacement estimation**

### **3.1 Introduction**

This chapter describes the followed methodology to estimate the displacements from the angular data of the bridge pier. The first part defines the steps followed to record the experimental data. The next part explains the characteristics of the input signals. The subsequent part defines the characteristics of the filters used to obtain the displacements from the recorded accelerations. Then, the calculations of errors of the estimation with respect to the LVDT are explained. Finally, the results are shown and analyzed.

### **3.2 Methodology**

#### **3.2.1 Total reference-free displacement**

The bridge displacement under train crossing events is composed of dynamic and pseudo-static components. The dynamic component is a zero-mean motion caused by the high frequency responses of the bridge under the vibration of the train. The deflection of the bridge at low frequencies caused by the non-symmetric effect of the weight of the train governs the pseudo-static displacement component. The accelerometers placed on the deck cannot capture the pseudo-static component of the displacement of the railroad bridge. To solve this problem, this research estimates the pseudo-static component using the relation between the inclination angle of the pile bent and its displacement.

For the preliminary validation of this experimental method, the pseudo-static displacement of the timber trestle piles is assumed to be governed by pure rocking

under trains. For this preliminary assumption and experimental validation, the time history of the angle will be directly proportional to the total displacement of the deck, which is the combination of pseudo-static and dynamic displacements. Equation (3.1) defines the trigonometric relation and Fig. 3.1 illustrates its application to railroad bridges.

$$d = \tan \alpha \cdot h \quad (3.1)$$

where  $h$  is the known height of the pier,  $\alpha$  is the inclination angle of the pier and  $d$  is the displacement of the deck.

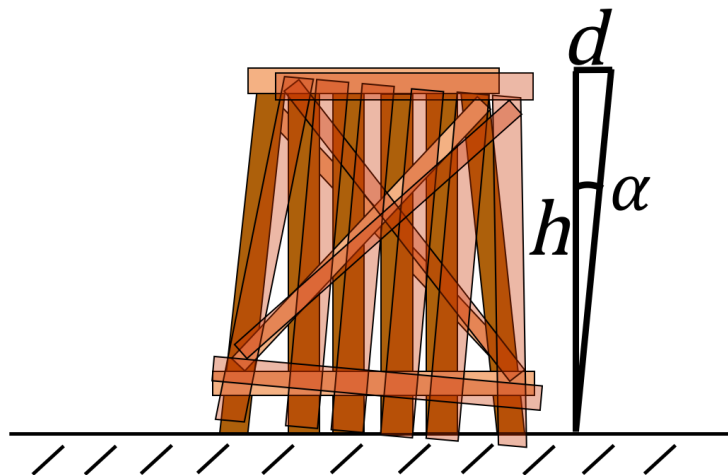


Fig. 3.1. Schematic relation between tilt and displacement of a railroad timber trestle.

### 3.2.2 Moving average filter for pseudo-static displacement estimation

This section describes the characteristics of the filter used to process the pseudo-static displacement measured from the inclination angle of the pile bent. Initially, a standard Kalman filter was employed to extract the trend of the angular data and eliminate the noise. The popularity a multiple application of Kalman filters

was the main reason why it was chosen at first. However, an unknown drift between the estimated pseudo-static displacement and the reference displacement appeared. Such drift varied depending on the nature of the original data and was not possible to compensate. Therefore, a moving average filter was utilized to extract the trend from the displacement obtained from the inclination angle. The conceived idea was to obtain the trend by calculating the mean of several points contained inside a predefined window and move that window along the data array to create multiple means from each window at every point. The optimal window size  $N$  was chosen to be half of the sampling frequency after performing an analysis on different window sizes. After the calculation of all the means resulting from the windows, the pseudo-static displacement was obtained averaging the means of the overlapping windows. Equation (3.2) shows the calculations performed to obtain the values of the filtered signal:

$$y(i) = \frac{1}{N} \sum_{j=0}^{N-1} x(i+j) \quad (3.2)$$

where  $x$  is the input data that is being filtered,  $y$  is the filtered output signal,  $i$  is the index of the analyzed point,  $N$  is the window size and  $j$  is the index of the point within the window. Fig. 3.2 graphically shows the process followed by the created filter. In Fig. 3.2 the behavior of the filter is illustrated. The window has a width  $N$ , which was determined to be half of the sampling rate. The window overlap was  $N-1$ , although the figure shows a smaller overlap for illustrative purposes. The mean of the data points contained inside the window,  $N$  is defined by  $M$  and the

mean of all the overlapping  $M$  returns the filtered data  $A$ . Fig. 3.2 illustrates that the filter can extract the trend despite the noise of the signal.

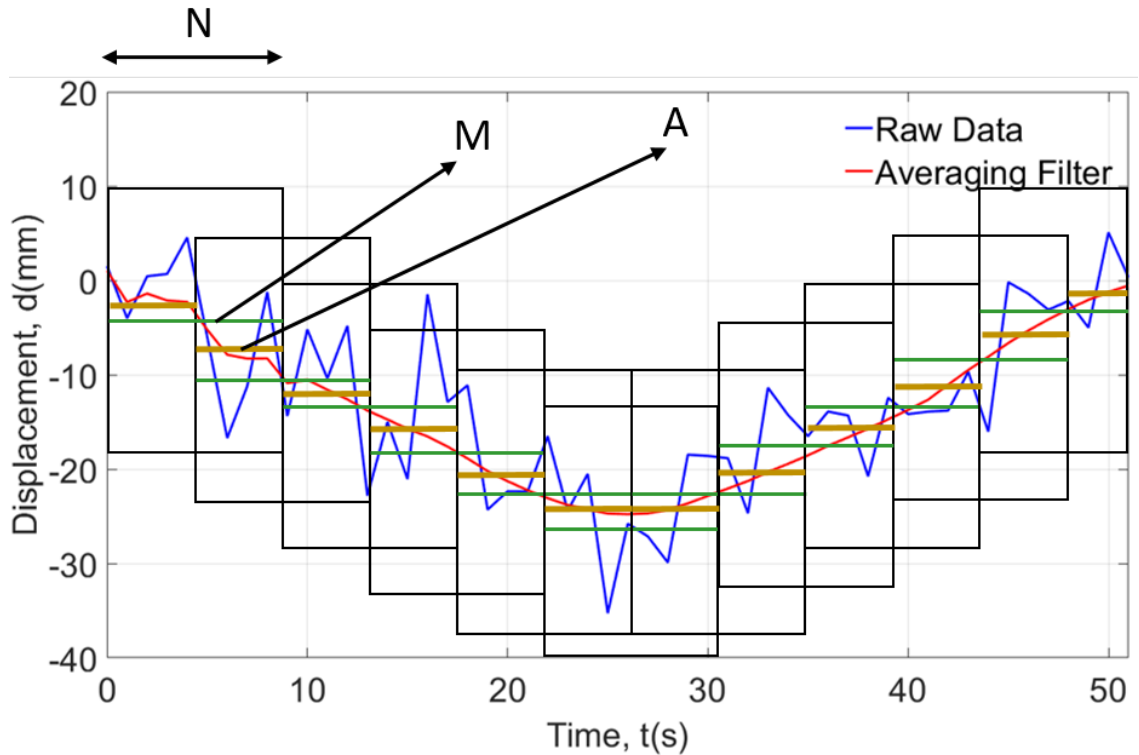


Fig. 3.2. Graphical demonstration of designed filter.

### 3.2.3 Performance evaluation criteria

Researchers calculated two types of errors to assess the error between the reference displacement measured by the LVDT and the estimations. The first performance index is the average peak error ( $E_1$ ):

$$E_1(\%) = \frac{\frac{\sum_{i=1}^n (A_i - B_i)}{n}}{\frac{\sum_{i=1}^n A_i}{n}} * 100\% \quad (3.3)$$

where: A is the maximum peak measured by the LVDT, B is the maximum peak of the displacement estimation and n is the number of points. This error value provides information regarding the behavior of the sensors when estimating the maximum points. This error considers the average of the differences in the data peaks between the estimations and the reference displacement.

The second performance index ( $E_2$ ) was the normalized Root Mean Square (RMS) error, which indicates the capability of the proposed methodology in capturing the overall nature of the displacements. The RMS error is calculated as given below:

$$RMSE = \sqrt{\frac{\sum_{i=1}^n (a_i - b_i)^2}{n}} \quad (3.4)$$

where  $a_i$  is the value of the reference displacement at a certain point at  $i^{\text{th}}$  time step,  $b_i$  is the value of the estimated displacement at the same point and  $n$  is the number of data points in the sample. Once the RMSE value is obtained, the second performance index ( $E_2$ ) can be written as follows:

$$E_2(\%) = \frac{RMSE}{A} \quad (3.5)$$

$E_1$  describes the ability of the estimation to determine the maximum displacements on the bridge.  $E_2$  defines an overall error percentage by comparing the estimation with the whole profile of the reference displacement.



### 3.2.4 Procedure overview

Once the researchers obtained the inclination angle, they calculated the displacement by substituting in equation (3.1). This method was not valid for estimating the total displacement accurately due to the noise of the measurements and therefore, the previously described moving average filter extracted the trend (i.e. pseudo-static component). To provide the remaining information, another accelerometer measured the acceleration of the shake table. Then, that acceleration was converted into the dynamic displacement by applying the previously described FIR filter. Researchers combined the two components of the displacement to obtain the total displacement estimation. Finally, the estimation error was quantified by comparing it to the reference displacement data collected by a LVDT. Fig. 3.3 shows the schematic methodology flow chart divided in four stages: data collection, data filtering, total displacement estimation and performance evaluation.

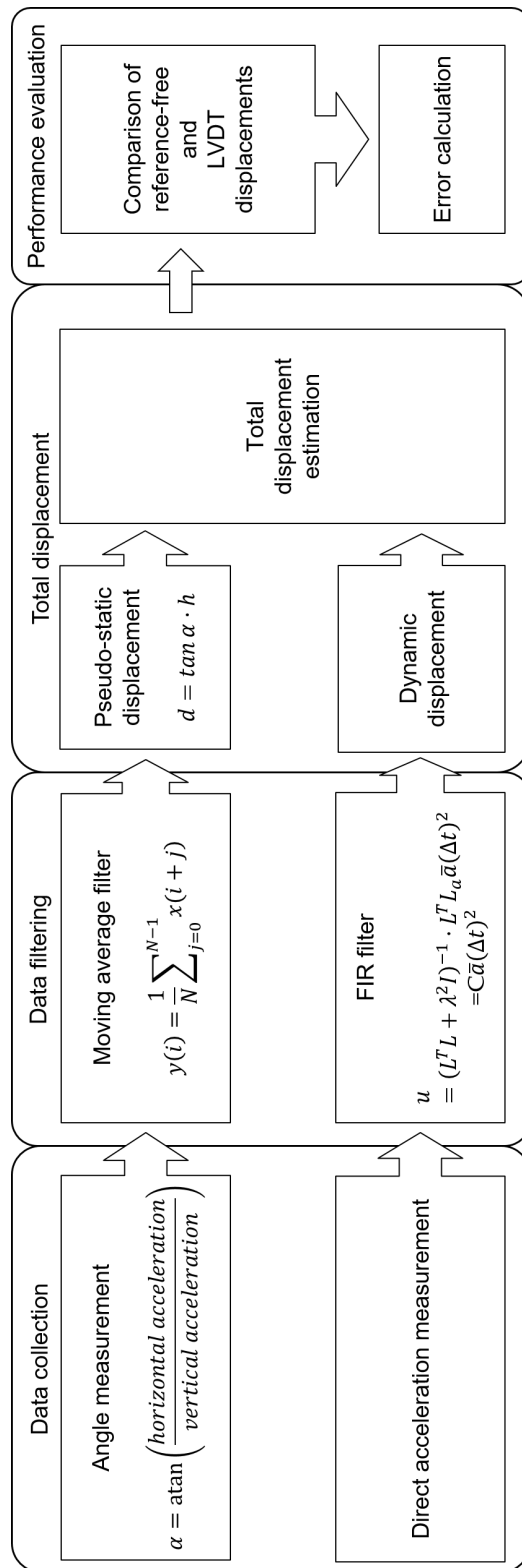


Fig. 3.3. Methodology of the tilt angle estimation from displacements.

### 3.3 Experiment

#### 3.3.1 Railroad bridge testing layout

This research proposes a new upside-down railroad bridge configuration to simulate the effect of train crossing on pile bents. The shake table acted as the vibrating railroad bridge deck. To provide a fixed ground for the base of the pile bent, researchers designed and built a steel frame on top of the shake table. The final design consisted of two tubes with different diameters that fitted inside one another allowing the differential elongation of the pile with respect to the frame. The tubes were pinned to the shake table and the fixed frame and were free to rotate with respect to the frame and the shake table respectively.

Two accelerometers placed on the vertical and horizontal direction measured the tilt angle of the pier. The calculation of the angle involves the readings of the two accelerometers with the tangent of the angle with respect to gravity as shown in equation (3.6).

$$\alpha = \text{atan} \left( \frac{\text{horizontal acceleration}}{\text{vertical acceleration}} \right) \quad (3.6)$$

Equation 3.6 combined the accelerations in the horizontal and vertical directions instead of relating only one of them with a sine or cosine function. The proof for this concept is shown in the equations (3.7) and (3.8) with a harmonic curve:

$$\alpha = \text{atan} \left( \frac{\text{horizontal position}}{\text{vertical position}} \right) = \text{atan} \left( \frac{X = A \cdot \cos wt}{Y = B \cdot \cos wt} \right) = \text{constant} \quad (3.7)$$

$$\begin{aligned} \alpha &= \text{atan} \left( \frac{\text{horizontal acceleration}}{\text{vertical acceleration}} \right) = \\ &= \text{atan} \left( \frac{X = -Aw^2 \cdot \cos wt}{Y = -Bw^2 \cdot \cos wt} \right) = \text{constant} \end{aligned} \quad (3.8)$$

Fig. 3.4 shows the final set-up for the measurement of tilt angles of railroad bridges.

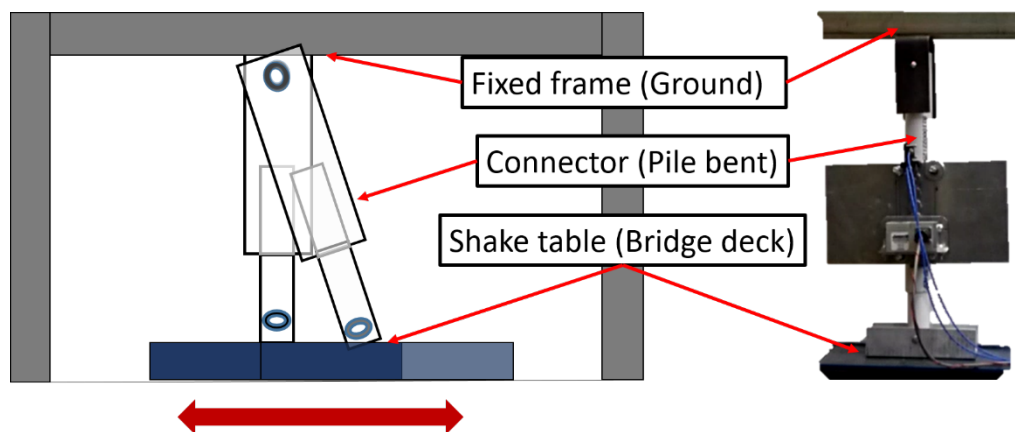


Fig. 3.4. Final set-up for railroad bridge tilt measurement.

### 3.3.2 Instrumentation

Two 3711B1110G capacitive accelerometers manufactured by PCB Piezotronics (PCB Piezotronics 2015) measured the tilt of the pile bent. The 3711E1110G is a capacitive MEMS DC accelerometer that can achieve true DC response for measuring uniform (or constant) acceleration. It has a sensitivity of 200 mV/g, a measurement range of  $\pm 10$  g and a frequency range from 0 to 1000 Hz. Additionally, another 3711B1110G accelerometer was attached to the shake

table in the direction of motion to record the dynamic component of the displacement. Fig. 3.5 shows the 3711B110G accelerometers used for testing.



Fig. 3.5. 3711B110G accelerometers close-up.

A linear variable differential transducer (LVDT), DCTH3000A manufactured by RDP Electrosense (RDP Electrosense 2016) collected the displacement of the shake table. This LVDT has a small linearity error (0.5 %) and a measuring range of  $\pm 75$  mm, which provides accurate readings to use it as the reference displacement. Output signals of all the sensors were sampled at a frequency of 1024 Hz with an 8-channel VibPilot DAQ system manufactured by M+P International (M+P International 2015). This DAQ has a 24-bit resolution A/D converters. A USB connected the VibPilot to a laptop computer for the control of sensing parameters such as the sensitivity of the sensors and their sampling frequency. Fig. 3.6 shows the used Vibpilot DAQ.



Fig. 3.6. Vibpilot Data Acquisition System.

The shake table used was a QUANSER Shake Table II (Quanser 2016), which allows a maximum displacement range of 15.2 cm. Fig. 3.7 shows the set-up.

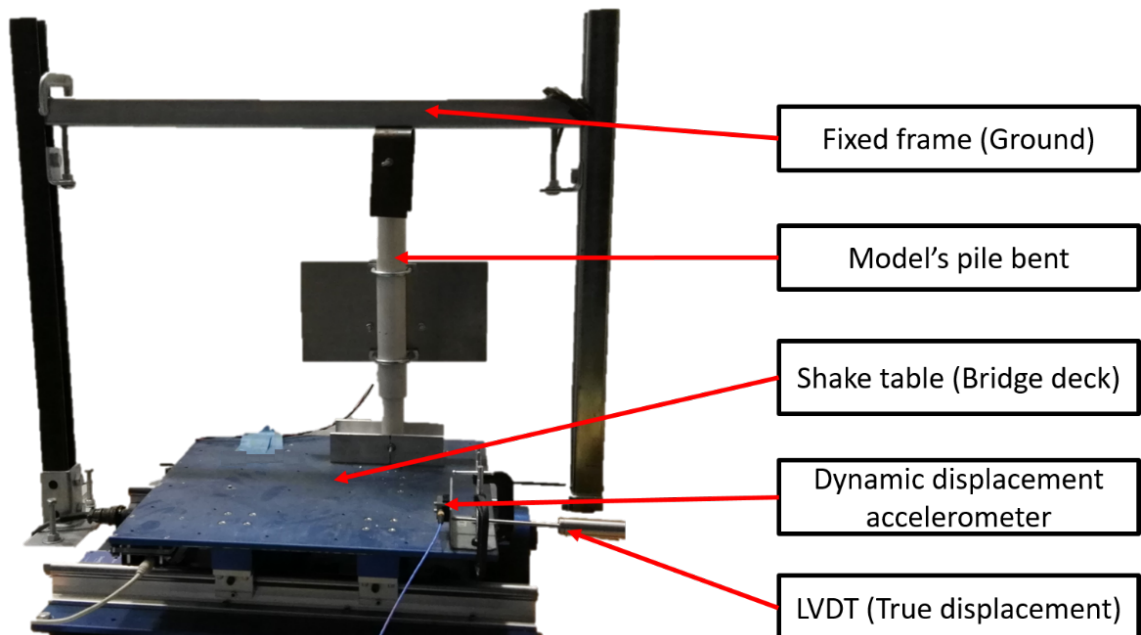


Fig. 3.7. Final set-up for railroad bridge tilt measurement.

### 3.3.3 Railroad bridge displacement data

To prove the efficiency of the method, ten different real bridge displacements were introduced with the shake table. The bridge displacements were taken during train crossings running at different speeds (ranging from 8.7 km/h to 41 km/h) and directions (northbound (NB) and southbound (SB)) (Moreu et al. 2015). Table 3.1 shows a detailed description of the train parameters.

Table 3.1. Train characteristics description.

Train	Speed,		Direction
	km/h	mph	
1	8.7	5.4	SB
2	8.7	5.4	NB
3	16.2	10.1	SB
4	17.8	11	NB
5	23.3	14.5	SB
6	24.9	15.5	NB
7	33.9	21	SB
8	31.1	19.3	NB
9	41.5	25.8	SB
10	41.0	25.5	NB

### 3.4 Experimental results

The ten different bridge displacements signals from the various train crossings described in the previous sections were inputted into the shake table. Researchers obtained the inclination angle of the pile bent by relating the components of the acceleration with a simple trigonometric relation as shown in equation (3.6). Then, the angular data was used to calculate the displacement relating it to the height of the pier as shown in equation (3.1). A moving average

filter extracted the pseudo-static component from the total displacement. Finally, the researchers combined the estimations of the dynamic and pseudo-static components to retrieve the total displacement estimation.

Fig. 3.8 displays the efficiency of the method to estimate total reference-free displacements under the 31.1 km/h northbound train. This train illustrates the effect of the harmonic rock and roll in the displacements. The harmonic rock and roll is an oscillatory motion associated with heavy cars and speeds around 24 km/h (Hussain et al. 1980). Railroad managers are interested in using displacement measurements to detect resonance of large trains (up to two miles of length) crossing timber trestles (Moreu et al. 2015). The repetitive loading of heavy loaded cards on long timber trestles can excite the rock and roll phenomena. According to the railroad, if total displacements could be measured with reference-free mean, those measurements could be used to inform railroads of the rock and roll resonance under different trains and speeds. The results shown in Figure 3.8 demonstrate the accuracy of the proposed method step by step.

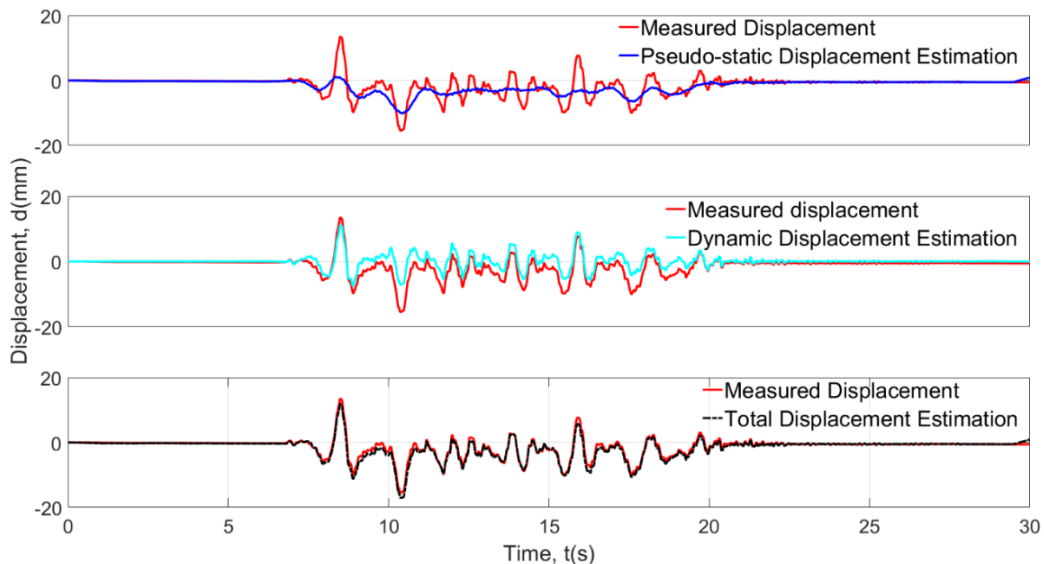


Fig. 3.8. Bridge displacement estimation under NB 3.1 km/h train.



Researchers followed the same process for the ten different train crossing events. Fig. 3.9 shows the pseudo-static displacement obtained from the tilt angle of the pile bent for all the trains. Fig. 3.10 presents the dynamic displacement estimations obtained from the displacement reconstruction algorithm explained in section 2.2.3 Finally, Fig. 3.11 shows the total displacement estimation after the combination of both components.

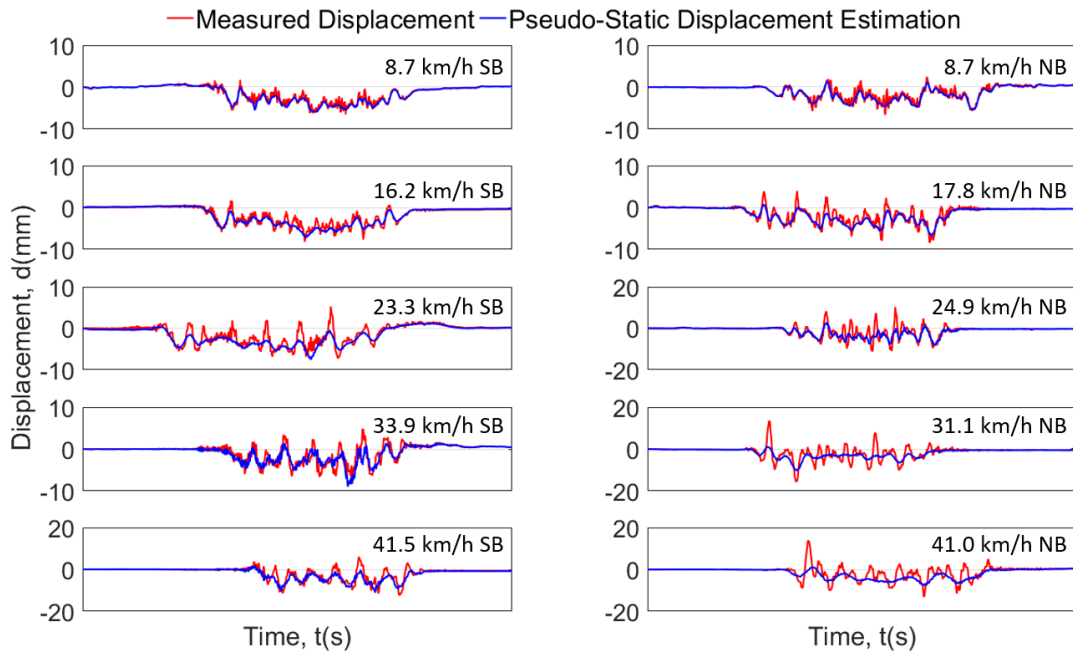


Fig. 3.9. Pseudo-static displacement estimation.

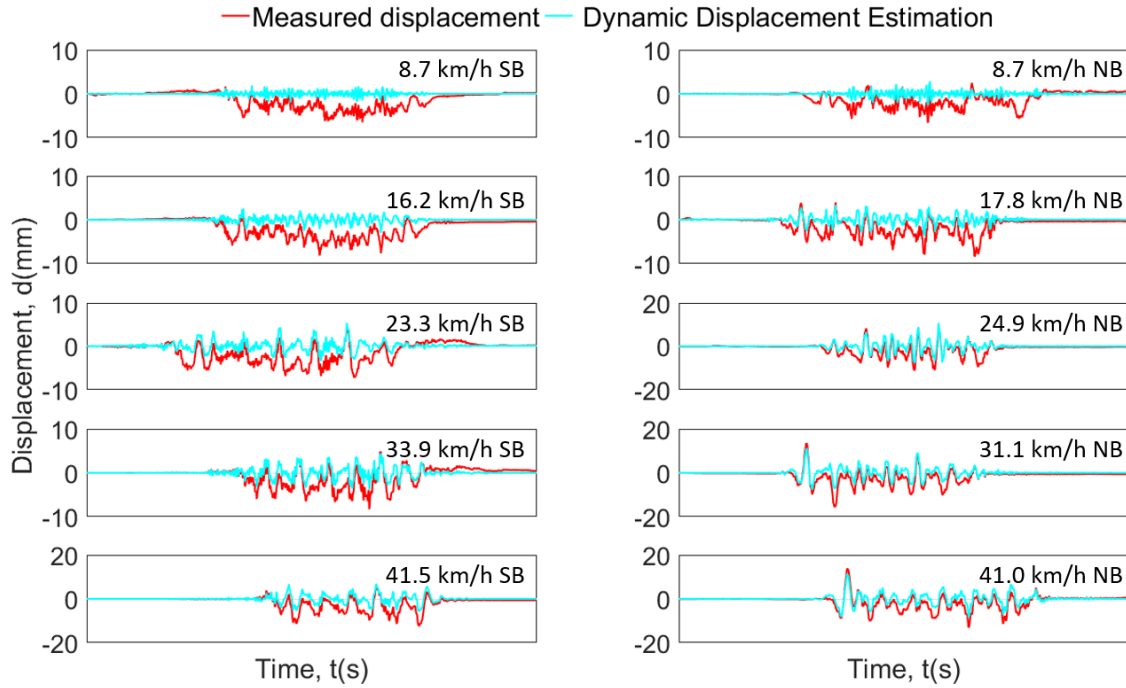


Fig. 3.10. Dynamic displacement estimation.

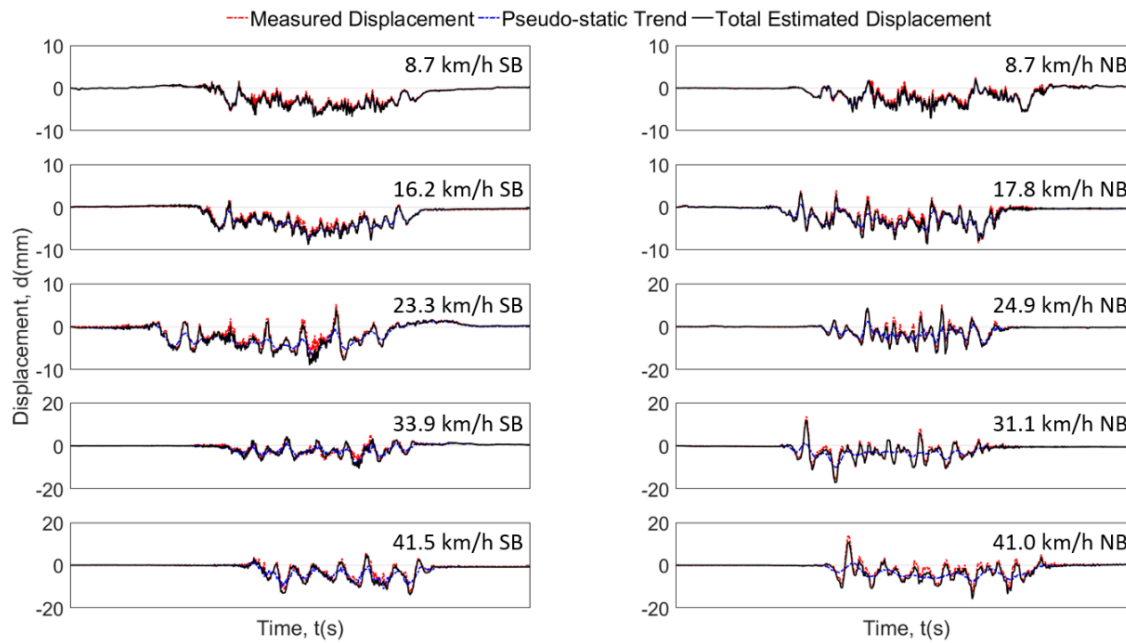


Fig. 3.11. Total displacement estimation.

Researchers obtained the time histories of the displacements and calculated the errors to quantify the accuracy of the implemented method. Fig. 3.12 displays the all-peak and root mean square errors obtained in the estimations of the ten train crossings.

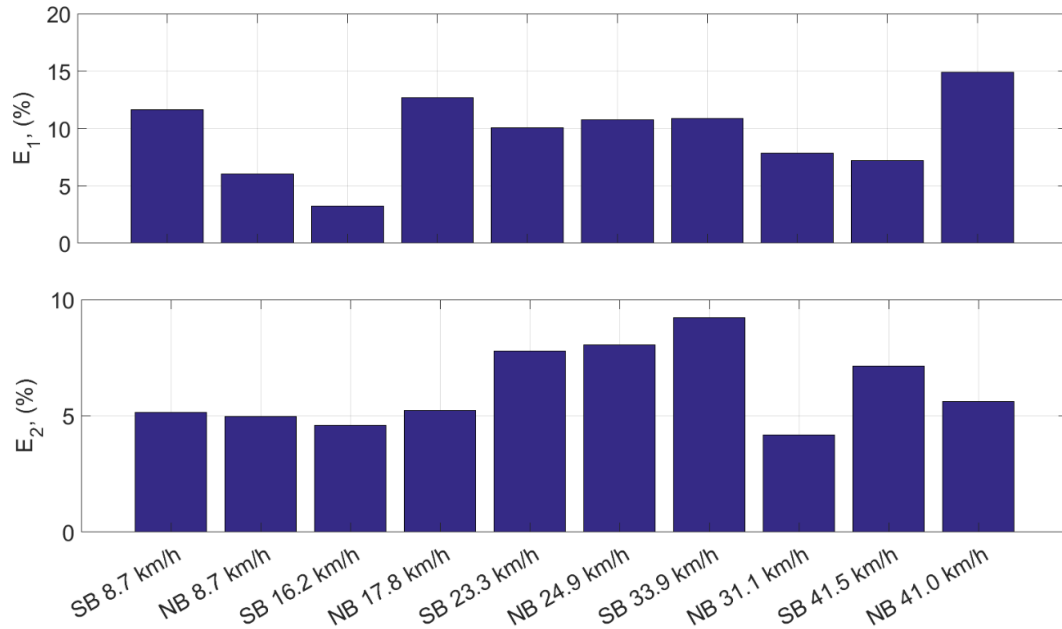


Fig. 3.12. Error values of the total displacement estimation.

Table 3.2 displays the error values for the two calculated performance parameters. With the exception of train 10, all the  $E_1$  errors are around 10 %. In the case of the  $E_2$  performance index, all the error values are below 10 %, being the average 6.2 %. The results show that the method is accurate and that it can effectively measure the transverse displacement of a railroad bridge without a fixed reference. Moreu et al. (2015) estimated the dynamic displacements of the same railroad bridge obtaining a 20 % error in average. The reference-free total displacement estimation method proposed in this paper obtained an average peak error of 9.52 % and a normalized RMS error of 6.2 %.

Table 3.2. Total displacement estimation errors.

Train	$E_1(\%)$	$E_2(\%)$
SB 8.7 km/h	11.65	5.14
NB 8.7 km/h	6.06	4.98
SB 16.2 km/h	3.26	4.60
NB 17.8 km/h	12.68	5.22
SB 23.3 km/h	10.03	7.79
NB 24.9 km/h	10.73	8.06
SB 33.9 km/h	10.89	<b>9.21</b>
NB 31.1 km/h	7.84	4.17
SB 41.5 km/h	7.21	7.14
NB 41.0 km/h	<b>14.87</b>	5.61

## **Chapter 4 Low-cost displacement estimation**

### **4.1 Introduction**

This chapter describes the experimental method to perform the low-cost estimation of the dynamic displacement of a railroad bridge model. This chapter includes the instrumentation, experimentation set-up, data processing, error calculation and result analysis. The chapter starts with the definition of the displacement estimation algorithm, then continues with the explanation of the characteristics of both the commercial and the low-cost accelerometers followed by a comparison in cost and capabilities between them. The next part consists on a description of the utilized set-up. Then, an explanation of the calculation methods is given. Finally, the results obtained are shown and discussed.

### **4.2 Methodology**

#### **4.2.1 Commercial sensing system**

This research used two different types of commercial sensors in the experimental process: (i) the 353B33 ICP accelerometer from PCB Piezotronics (PCB Piezotronics 2015), a single- axis piezoelectric accelerometer with a fixed voltage sensitivity of 100 mV/g, a measurement range of  $\pm 50$  g, a frequency range from 1 to 4000 Hz and (ii) the 3711E1110G PCB Capacitive microelectromechanical system (MEMS) DC accelerometer (PCB Piezotronics 2015) that can achieve true DC response for measuring uniform (or constant) acceleration and measure low-frequency vibration. It has a sensitivity of 200 mV/g,

a measurement range of  $\pm 10$  g, and a frequency range from 0 to 1000 Hz. Fig. 4.1 shows an image of the 353B33 ICP accelerometer.

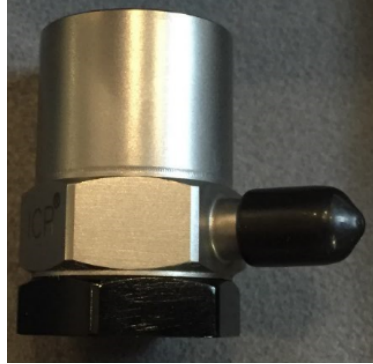


Fig. 4.1. 353B33 ICP accelerometer close-up.

The previously described Vibpilot data acquisition system was used to obtain readings from the sensors. A USB cable provided the connection between the VibPilot and a laptop to control the sensing parameters such as the channels used, the sensitivity of the sensors and the sampling frequency. After the data collection, the computer saved it as a MATLAB software data file for post-processing (MATLAB 2015).

#### **4.2.2 Low-cost sensing system**

An Arduino Uno and a low-cost accelerometer formed the low-cost system. The Arduino Uno board is a low-cost low-power microcontroller that acts as the data acquisition system (DAQ). The Arduino Uno board has an operating voltage of 5V, 14 digital input/output pins, and 6 analog input/output pins. A USB cable or an external power supply (i.e. an AD-to-DC adapter or a battery) can power the

Arduino board. Arduino is an open-source prototyping platform that offers a variety of possibilities from everyday objects to complex scientific instruments. Its versatility and easiness in pairing with other sensors such as accelerometers, gyroscopes or magnetometers, besides its wide availability in the market for the end consumer, determined the choice of the model. In addition, Arduino has its own development environment that supports a C-based programming language allowing users to configure the performance of the microcontroller without restrictions. The user can upload the generated programs to the Arduino board via USB connection.

To provide railroad and infrastructure owners with a low-cost sensor that can be used for reference-free displacements, researchers tested three low-cost accelerometers. First, researchers chose a low-cost accelerometer called ADXL345, an ultra-low power digital accelerometer manufactured by Analog Devices (Analog Devices 2015a). The ADXL345 accelerometer has a user-selectable resolution ranging from 10 to 13 bits and a variety of measuring ranges of  $\pm 2$  g,  $\pm 4$  g,  $\pm 8$  g and  $\pm 16$  g with a minimum scale factor of 4 mg/Least-Significant-Bit (LSB), depending on the selected range. The second sensor was the ADXL362, also manufactured by Analog Devices (Analog Devices 2015b). This accelerometer has a resolution of 1 mg/LSB, which provides a sensitivity four times higher than the ADXL345, and a selectable measurement range of  $\pm 2$  g,  $\pm 4$  g, and  $\pm 8$  g. In addition, the ADXL362 accelerometer has many features to enable true system power reductions. It has a sleep operation mode to save power when there are not any excitations that have to be measured. Finally, researchers tested the

MMA8452Q, a capacitive accelerometer manufactured by NXP Semiconductors (NXP Semiconductors 2015). This accelerometer has less than 1 mg/LSB sensitivity with selectable measurement ranges  $\pm 2$  g,  $\pm 4$  g, and  $\pm 8$  g. The MMA8452Q has low-pass filters to avoid unwanted high frequencies and is a low-power consumption device. Fig. 4.2 shows an image of the three low-cost accelerometers.

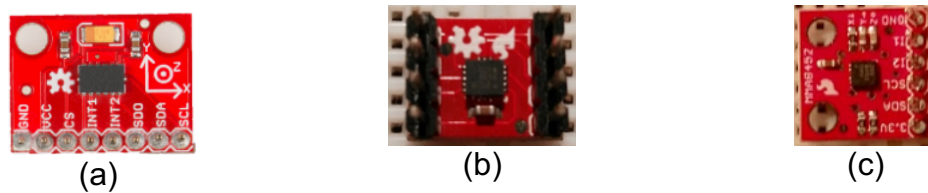


Fig. 4.2. Low-cost accelerometers (a) ADXL345, (b) ADXL362, (c) MMA8452Q.

To sum up, the three different low-cost accelerometers have features and characteristics that can be useful for accurate displacement estimations. While ADXL345 has some built-in features such as tap or freefall detectors and four adjustable measurement ranges, its sensitivity is as high as 3.9 mg/LSB, which limits the ability of the sensor to capture small changes. On the other hand, both ADXL362 and MMA8452Q have a higher sensitivity (approximately 1mg/LSB), but some of the characteristics that are present in the ADXL345 are not in these two. In addition, there are less range selection possibilities (maximum of  $\pm 8$ g). However, for the desired applications, these sensors might not need higher acceleration ranges to measure accelerations of larger amplitude. All of the low-cost sensing solutions have the potential to obtain power from independent sources such as batteries, DC power supplies or solar pannels due to their low



power consumption. Fig. 4.3 shows an image of the connection between an Arduino and an accelerometer.

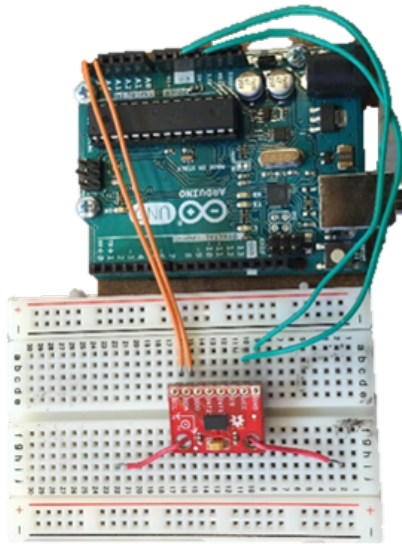


Fig. 4.3. Arduino UNO and ADXL345 accelerometer.

#### **4.2.3 Low-cost and commercial sensing systems comparison**

Table 4.1 displays a comparison between the cost of the commercial and the low-cost sensors (including the price of the acquisition systems used in the experiments). The table shows the price differences between the two sensing systems. Low-cost sensing systems are about 300 times less costly than the commercial alternatives. The low-cost sensing systems have a lower sampling rate when compared to the commercial sensors. The sampling rate determines the number of data points taken per second. If the sampling rate is not high enough there might be significant data losses between measurements. The sensitivity reflects the relation between the smallest measured unit and the output. It is an indicator of the level of precision of the sensor. If there are small changes in the measurements during the data acquisition, a sensor with an insufficient sensitivity

will not capture such changes. In addition, the sensors are also characterized by another parameter called resolution. The resolution indicates the smallest physical change that can be detected by the sensor, which is strictly related to the phenomenon of quantization. The quantization of a signal is the transformation of a physical event into discrete measurable information. The accuracy of that quantization depends on the number of levels that the signal is divided into. Sensors are in charge of that discretization and the number of levels is defined by the resolution. If the resolution is not sufficient to capture the physical event, the signal gets truncated and quantization errors appear. The better the sensor is (and usually more expensive too), the highest resolution it has. Fig. 4.4 illustrates the quantization errors of the used sensors on a simulated sinusoidal wave. Fig. 4.4 shows the difference in resolution of the two commercial and the three low-cost accelerometers.

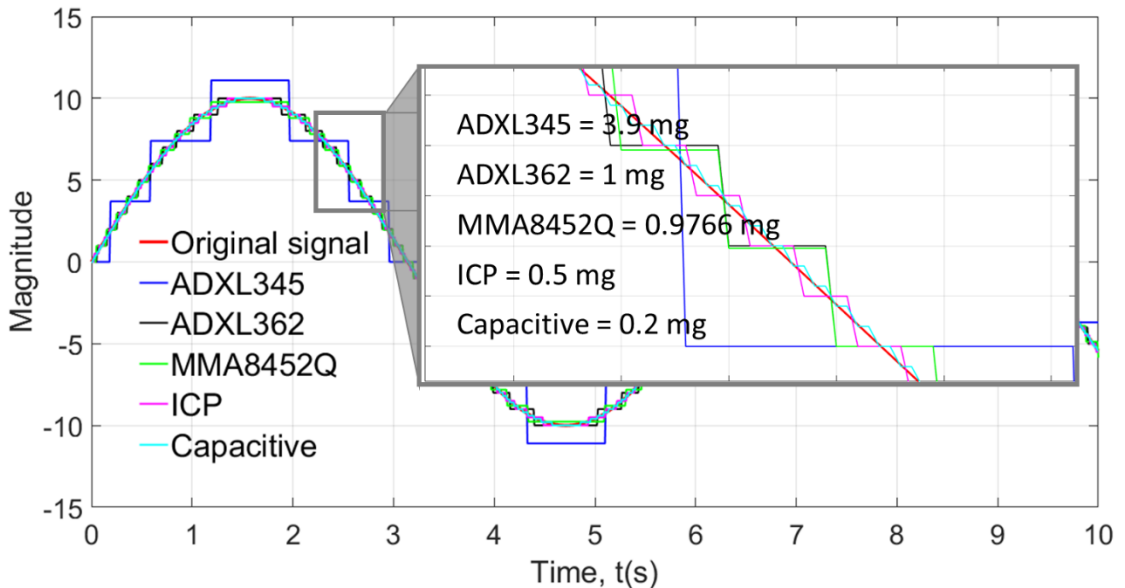







Fig. 4.4. Quantization errors of the used accelerometers.

There are also other aspects that can determine the sensor performance such as the signal to noise ratio or the effect of the temperature on the quality of the readings. Usually, the signal to noise ratio varies linearly with respect to the output data rate and the bandwidth. Generally, the better the sensor is, the less affected it is by noise. The signal to noise ratio is usually expressed in  $\frac{\mu g}{\sqrt{Hz}}$  units, which can be traduced to bits using the resolution and introducing the output data rate. In the case of the ADXL345 the signal to noise ratio at 100 Hz output data rate is  $412 \frac{\mu g}{\sqrt{Hz}}$  for x and y axes and  $606 \frac{\mu g}{\sqrt{Hz}}$  for the z axis. In the case of the ADXL362 it is  $550 \frac{\mu g}{\sqrt{Hz}}$  for the x and y axes and  $920 \frac{\mu g}{\sqrt{Hz}}$  for the z axis. Similarly the signal to noise ratio of the MMA8452Q low-cost sensor is  $126 \frac{\mu g}{\sqrt{Hz}}$  for all axes. On the other hand, the 353B33 ICP accelerometer has a signal to noise ratio ranging from 320 to  $6.4 \frac{\mu g}{\sqrt{Hz}}$  being inversely proportional to the output data rate. The 3711E1110G has a signal to noise ratio of  $107.9 \frac{\mu g}{\sqrt{Hz}}$ . This data shows that although the low-cost sensors are in general more sensitive to noise, there is not that much of a difference between the two types. This fact is due to the bigger range of frequencies that commercial accelerometers can provide. In addition, the quality of the data taken by the sensors is affected by temperature. In this research, that drift due to temperature was ignored due to the ideal temperature conditions of the laboratory. However, this factor would have to be considered for field experimentation.

Table 4.1. Sensor cost comparison.

Sensor			Sensitivity		DAQ	Sampling Rate (Hz)	Cost		
Name	Maker	Weight (g)	Analog (mV/g)	Digital (LSB/g)			Sensor (\$)	DAQ (\$)	Total (\$)
 3711B1110G (Capacitive)	PCB Piezotronics	16.3	201.1	N.A.	Vibpilot-8	1024	13,600.00	724.00	14,315.00
 353B33 (ICP)	PCB Piezotronics	27.0	101.9	N.A.	Vibpilot-8	1024	13,600.00	320.00	13,911.00
 ADXL345	Analog Devices	0.02	N.A.	256	Arduino Uno	100	25.00	18.00	43.00
 ADXL362	Analog Devices	0.02	N.A.	1000	Arduino Uno	100	25.00	15.00	40.00
 MMA8452Q	NXP Semiconductors	0.02	N.A.	1024	Arduino Uno	200	25.00	10.00	35.00

#### 4.2.4 Experiment set-up

The shake table QUANSER Shake Table II (Quanser 2016) provided the railroad bridge excitations. This shake table consists of a top stage driven by a powerful servo-motor that reproduces vibrations. A DCTH3000A LVDT manufactured by RDP Electrosense (2016) measured the shake table displacements. This LVDT has a linearity error of 0.5 % and a measuring range of  $\pm 75$  mm. Accelerometers (both commercial and low-cost) measured the accelerations caused by the shake table. Fig. 4.5 shows an image of the experimental set-up including the shake table, the LVDT, the commercial ICP sensor and two Arduino Uno boards along with the low-cost accelerometers.

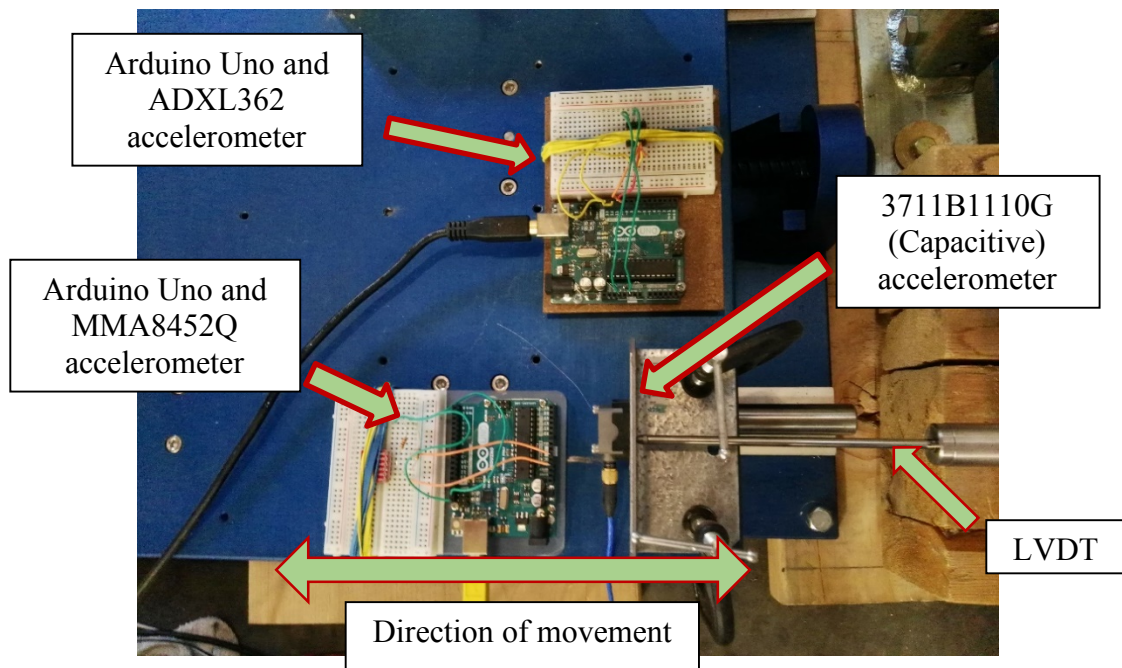


Fig. 4.5. Displacement estimation experimental set-up (plan view from above).

#### 4.2.5 Experimental methodology

Researchers conducted experiments using low-cost and commercial accelerometers using the shake table to prove the effectiveness and accuracy of low-cost sensors for SHM of railroad bridges,. The experiments consisted of measuring the acceleration of the shake table and using the previously described FIR filter to reconstruct the dynamic displacement. The shake table was actuated with three different types of excitations. The first experiment was a series of six cyclic sine waves. The second experiment included three earthquake signals. The third experiment reproduced real train excitations measured on the field. Researchers collected the accelerations with accelerometers and the reference displacements using the LVDT. Finally, the researchers compared the displacement estimations from both low-cost and commercial accelerometers with the LVDT measurements to calculate the errors. The three types of performance indexes computed with the different errors are described in the next section. Fig. 4.6 illustrates the experiment methodology pursued in all the tests.

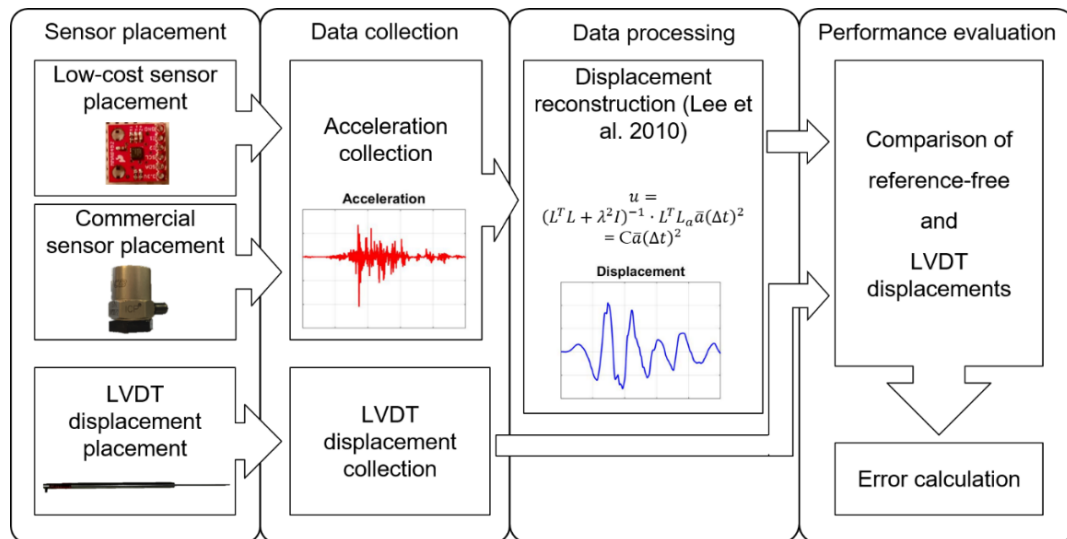


Fig. 4.6. Experimentation methodology flow chart.

#### 4.2.6 Performance evaluation criteria

Researchers used three different performance indices to quantify the error between the displacement estimations and the reference displacement measured by the LVDT.

The first performance index is the maximum peak error ( $E_1$ ):

$$E_1(\%) = \frac{A - B}{A} * 100\% \quad (4.1)$$

where  $A$  and  $B$  are the absolute maximum peak displacements measured by the LVDT and estimated by the accelerometer, respectively. This error index quantifies the error of reference-free sensors estimating the maximum peak displacement under dynamic movements, regardless of the location of this maximum peak throughout the time history of the signal.

The second performance index is the average peak error ( $E_2$ ):

$$E_2(\%) = \frac{\frac{\sum_{i=1}^n (A_i - B_i)}{n}}{\frac{\sum_{i=1}^n A_i}{n}} * 100\% \quad (4.2)$$

where  $A$  and  $B$  denote the peaks of the measured and estimated displacement respectively and  $n$  corresponds to the number of peaks considered. The differences in the peaks between all the maxima and minima in the displacements were averaged to obtain the average peak error ( $E_2$ ).

To calculate the third performance index, the RMS error has to be calculated first:

$$RMSE = \sqrt{\frac{\sum_{i=1}^n (a_i - b_i)^2}{n}} \quad (4.3)$$

being  $a_i$  the value of the reference displacement (LVDT) at  $i^{\text{th}}$  time step,  $b_i$  the value of the estimated displacement and  $n$  is the total number of data points.

Finally, the third performance index is the normalized Root Mean Square Error ( $E_3$ ), given by the equation:

$$E_3(\%) = \frac{RMSE}{A} \quad (4.4)$$

The RMS error value is then normalized by dividing it by the maximum peak of the reference displacement  $A$ .

$E_1$  determines the accuracy of the estimation of the maximum peak,  $E_2$  describes the ability of the estimation to determine the maximum displacements on the bridge and  $E_3$  gives an overall error percentage by comparing the estimation with the whole profile of the reference displacement.

### 4.3 Experiments and results

In this section the experimental results are presented. The approach followed was to input more realistic train excitations successively. The first test represented a simplified bridge excitation in the form of sinusoidal waves, then



earthquake motions and train excitations were simulated respectively. This section displays the results in the previously defined order.

#### 4.3.1 Uniform sinusoidal excitation

Firstly, researchers estimated reference-free displacements using six different sinusoidal waves (Table 4.2). Based on the maximum transverse displacement values of railroad bridges under traffic conditions measured by Moreu et al. (2014), the amplitudes were designed to be from 6.35 to 19.05 mm (0.25 to 0.75 in). Similarly, this experiment run sinusoidal tests with 1 and 2 Hz frequency based on standard railroad bridge responses (Moreu et al. 2014).

Table 4.2. Description of sinusoidal wave excitation characteristics.

Sinusoidal wave	Frequency, Hz	Amplitude,	
		mm	in
1	1	6.35	0.25
2	1	12.7	0.5
3	1	19.05	0.75
4	2	6.35	0.25
5	2	12.7	0.5
6	2	19.05	0.75

Researchers calculated the displacement estimation of the three low-cost accelerometers and one commercial accelerometer (Capacitive). Fig. 4.7 shows a sample of the estimations of the MMA8452Q and the Capacitive 3711B1110G (Capacitive) accelerometer with respect to the LVDT displacement measurements. The error values obtained are a result of subtracting the estimation from the

reference displacement of the LVDT. Figure 4.7 displays the estimation for the 2 Hz and 19.05 mm sine wave.

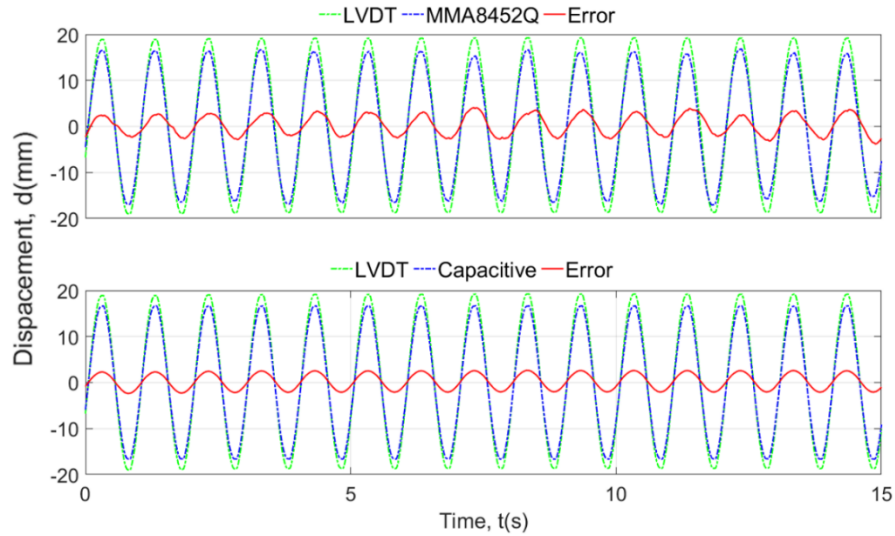


Fig. 4.7. Displacement estimation comparison for MMA8452Q and Capacitive to LVDT.

Fig. 4.8 displays the errors of the ADXL345 and ICP sensors. It also shows that the error coefficient  $E_3$  is very similar for both the commercial and the low-cost accelerometers. The maximum value of  $E_1$  is 44.92 % and of  $E_3$  is 18.02 %. The ADXL345 low-cost accelerometer had high quantization error due to its insufficient resolution, which explains some of the high error percentages.

Fig. 4.9 shows the errors obtained from the estimation of the ADXL362 low-cost accelerometer and ICP. The ADXL362 provided a higher resolution and improved performance with respect to the ADXL345. In this estimation, the maximum  $E_1$  error value is 24.93 % and the maximum  $E_3$  is 12.90 %. An improvement with respect to the previous estimation can be observed although the  $E_1$  error value is higher than acceptable.

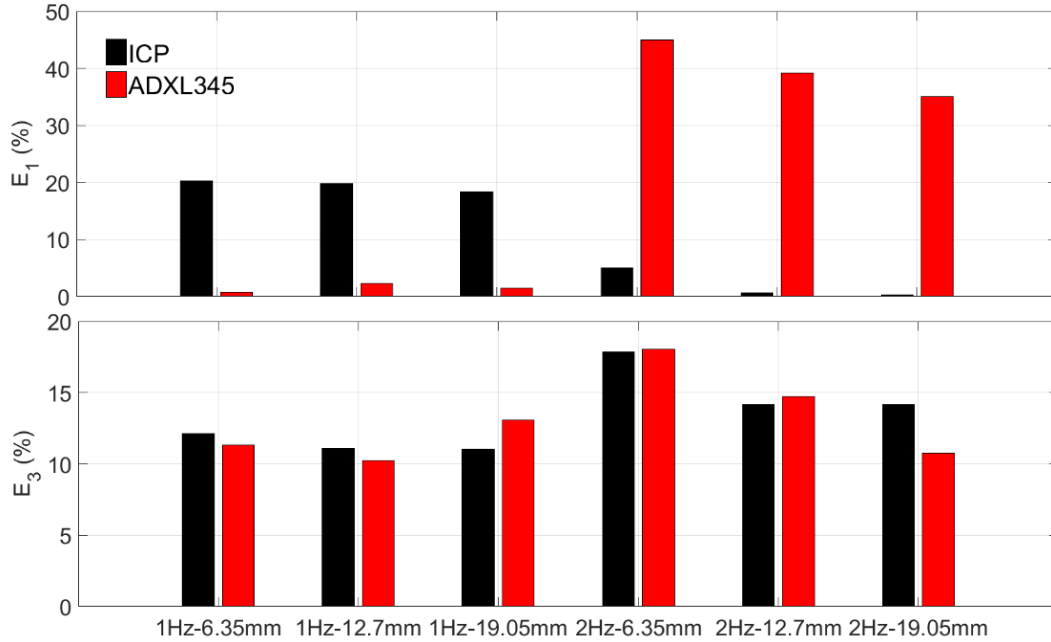


Fig. 4.8. Error values for ADXL345 vs ICP for sine wave tests.

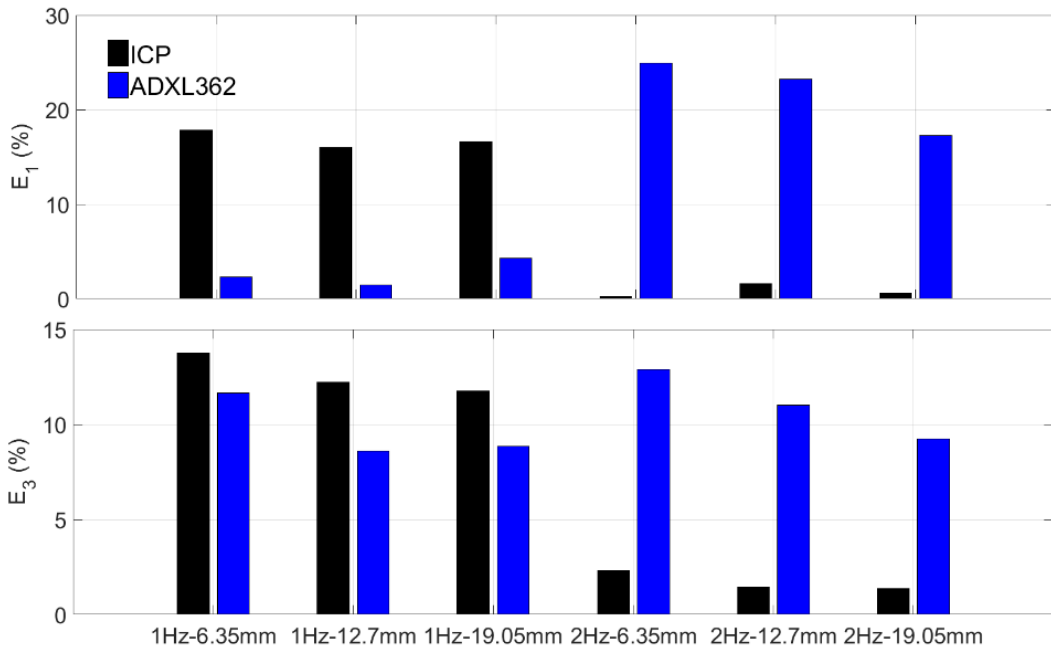


Fig. 4.9. Error values for ADXL362 vs ICP for sine wave tests.

For the last estimation, the used commercial sensor was the 3711E1110G (Capacitive) instead of the ICP. Fig. 4.10 displays the error values obtained with the MMA8452Q low-cost sensor and Capacitive. The MMA8452Q low-cost accelerometer was also used due to its higher resolution compared to the first

accelerometer (ADXL345) and to provide a comparison with the ADXL362 low-cost accelerometer. In this case, the error values decreased again, being the maximum  $E_1$  value 20.28 % and  $E_3$  11.47 %. With the exception of the 2 Hz error values for  $E_1$ , the low-cost estimation is similar and in some cases better than the Capacitive.

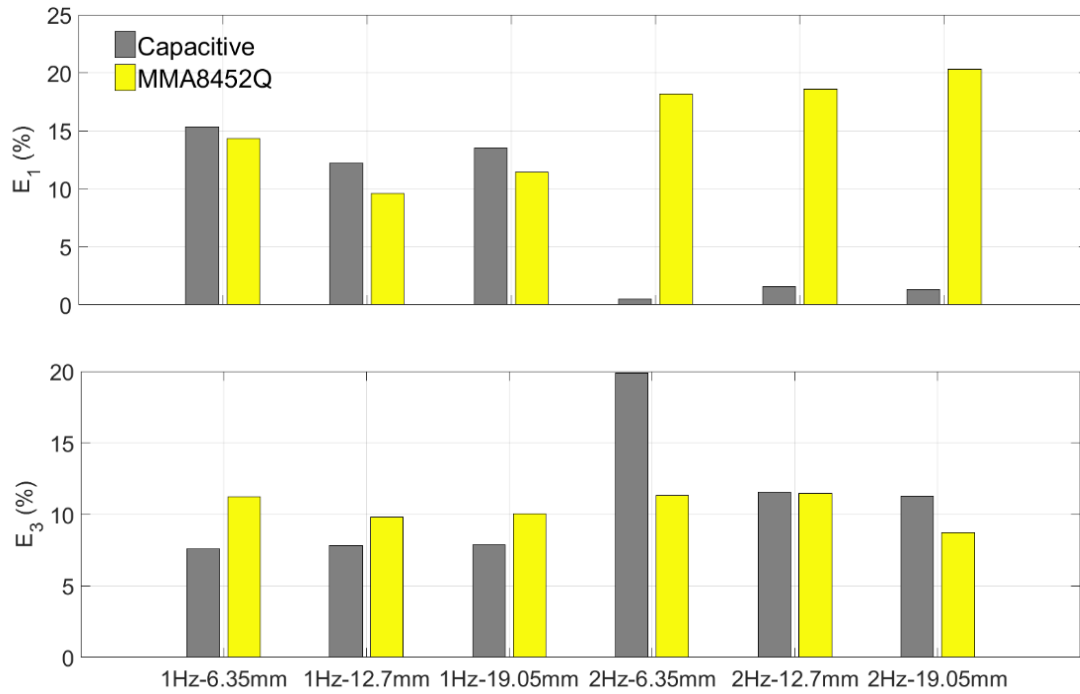


Fig. 4.10. Error values for MMA8452Q vs Cap for sine wave tests.

Fig. 4.11 shows the comparison of all the low-cost estimations. Table 4.3 shows the numerical values of the calculated errors with the maximum errors of each input signal in bold. In the case of the 1 Hz sinewave, the maximum peak errors of the low-cost sensors are less than 15 %, which is less than the estimation using commercial accelerometers. In the case of the 2 Hz sinewave, the maximum peak errors of the low-cost sensors ADXL362 and the MMA8452Q are less than 25 % and 21 %, respectively. In the case of the root mean square errors, the

deviations were nearly 10 % in all the cases, MMA8452Q and ADXL362 being superior in most comparisons.

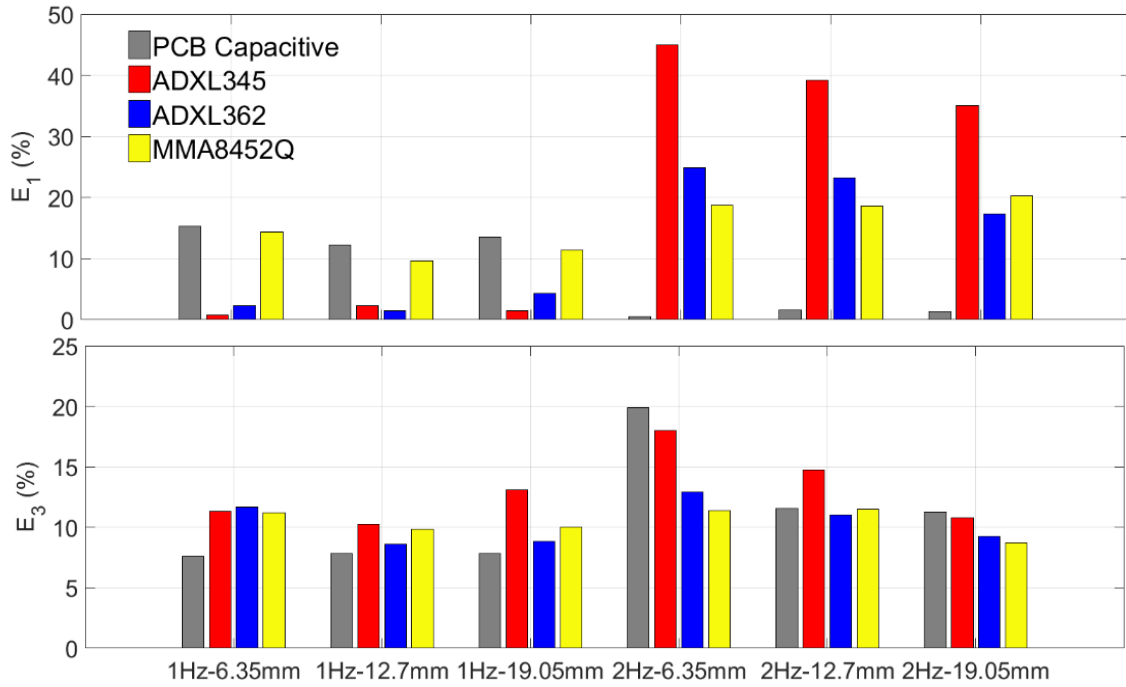


Fig. 4.11. Comparison of errors of the displacement estimations.

Table 4.3. Uniform sinusoidal excitation errors.

Sine Wave	$E_1$ (%)				$E_3$ (%)			
	Cap	345	362	MMA	Cap	345	362	MMA
1Hz - 6.35mm	- <b>15.36</b>	-0.74	2.31	-14.35	7.59	11.33	<b>11.66</b>	11.22
1Hz - 12.7mm	<b>12.17</b>	2.27	1.42	-9.60	7.81	<b>10.26</b>	8.60	9.82
1Hz - 19.05mm	<b>13.51</b>	-1.46	4.32	-11.44	7.85	<b>13.09</b>	8.84	10.03
2Hz - 6.35mm	0.50	<b>44.92</b>	24.93	18.74	<b>19.87</b>	18.02	12.90	11.40
2Hz - 12.7mm	1.56	<b>39.20</b>	23.24	18.61	11.56	<b>14.75</b>	11.03	11.47
2Hz - 19.05mm	1.30	<b>35.03</b>	17.27	20.28	<b>11.28</b>	10.76	9.26	8.70

Table 4.3 displays the error percentages for the sinusoidal displacement estimations. In each case, the numbers in bold highlight the highest error value for a specific sine wave test and evaluation criteria among the three sensors. Table 4.3 shows that the estimations provided by the ADXL345 are higher than the rest of the sensors in almost all the cases. However, the estimations of both the ADXL362 and the MMA8452Q are comparable to the ones obtained with the commercial sensor. The RMS error values are similar to the commercial in all cases, being always between 8 and 13 %. The ADXL345 was not used for displacement estimations under earthquakes and train crossing events.

#### **4.3.2 Earthquake displacement estimation**

Researchers tested the ability of low-cost sensors to estimate the displacement from three past earthquake records: El Centro 1940, Northridge 1994, and Cape Mendocino 1992. Researchers excited the shake table with the earthquake displacements. To show the results of these experiments, researchers used the previously described performance indices. In these cases, the error value  $E_2$  was used instead of  $E_1$ . Fig. 4.12 shows the reference-free dynamic displacement estimation of El Centro earthquake using both types of sensors. Figure 4.12 shows that the reference-free displacement estimations of low-cost and commercial sensors are similar in the time-domain, in particular the MMA8452Q. The error assessment is calculated in the following section.

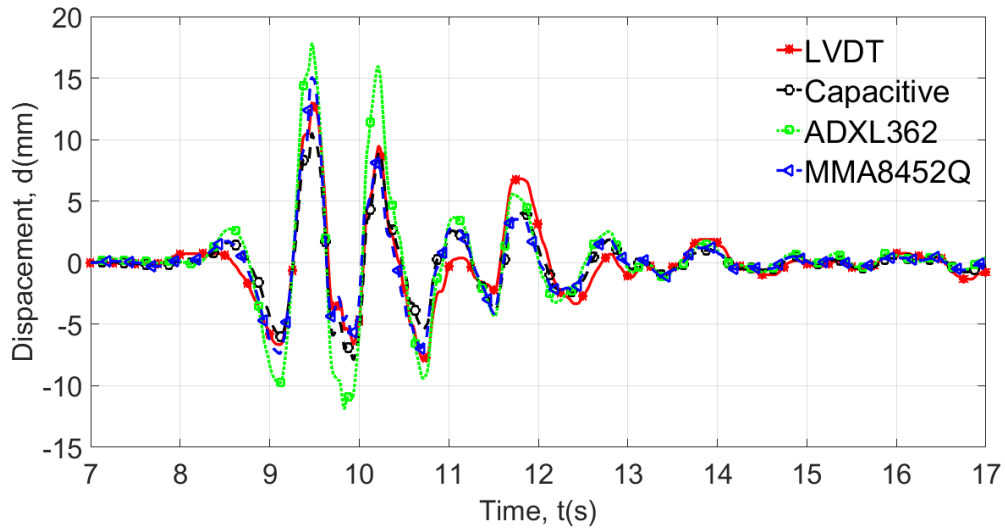


Fig. 4.12. El Centro earthquake displacement estimation.

Researchers calculated the errors between the displacement estimations and the reference LVDT displacements measured from three earthquakes using the shake table. Fig. 4.13 shows performance indices  $E_2$  and  $E_3$ .

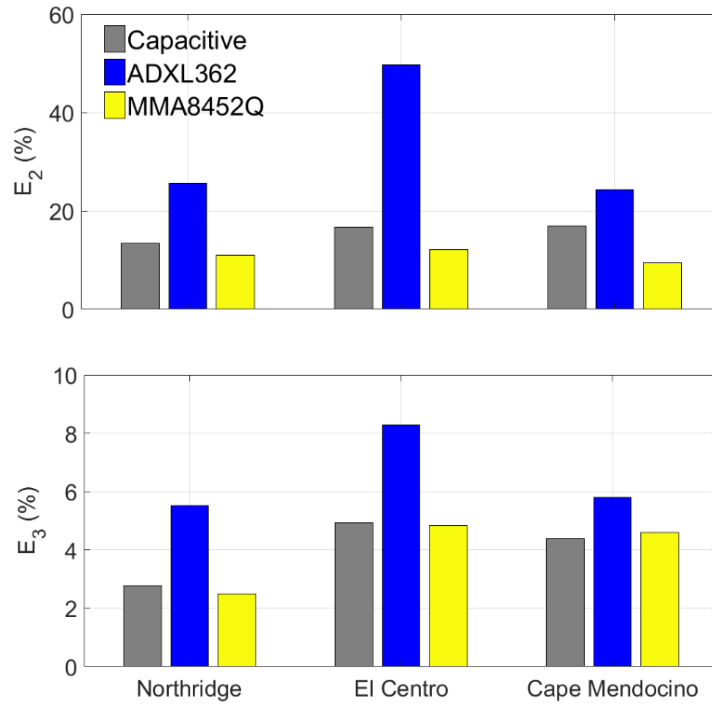


Fig. 4.13. Error values for Capacitive vs ADXL362 vs MMA8452Q for earthquake tests.

Table 4.4 displays the numerical errors for the earthquake simulations. The table shows the error percentages for  $E_2$  and  $E_3$ . For all three earthquakes, the  $E_2$  error using the MMA8452Q (low-cost) is less than the error of the Capacitive (commercial). Similarly, for all three earthquakes the  $E_3$  error is always below 9 %, and below 5 % for the MMA8452Q (low-cost) accelerometer.

Table 4.4. Earthquake displacement estimation error.

Earthquake	$E_2$ (%)			$E_3$ (%)		
	Capacitive	ADXL362	MMA8452Q	Capacitive	ADXL362	MMA8452Q
Northridge	13.39	<b>25.55</b>	10.93	2.78	<b>5.51</b>	2.50
El Centro	16.64	<b>49.71</b>	12.18	4.94	<b>8.27</b>	4.85
Cape Mendocino	16.98	<b>24.28</b>	9.38	4.38	<b>5.81</b>	4.60

Table 4.4 shows that the error values obtained for the earthquake simulations. The bold results indicate that the errors from the ADXL362 estimations are consistently higher than the errors obtained with the other sensors. The maximum value for  $E_2$  was 49.71 % while the maximum value for  $E_3$  was 8.27 %. On the other hand, the estimations of the MMA8452Q are better than the commercial ones in almost every case, which demonstrates the potential of the method.



### 4.3.3 Train displacement estimation

Researchers used the shake table to run bridge transversal displacements measured on the field. The real bridge displacements used for these experiments were taken from Moreu et al. (2015). The speed and direction of the trains varied as shown in table 4.5. This experiment consisted on five southbound (SB) trains and five northbound (NB) trains.

Table 4.5. Train characteristics description.

Train	Speed,		Direction
	km/h	mph	
1	8.7	5.4	SB
2	8.7	5.4	NB
3	16.2	10.1	SB
4	17.8	11	NB
5	23.3	14.5	SB
6	24.9	15.5	NB
7	33.9	21	SB
8	31.1	19.3	NB
9	41.5	25.8	SB
10	41.0	25.5	NB

Researchers used the same experiment set-up and considered errors  $E_2$  and  $E_3$ . Fig. 4.14 shows the reference-free dynamic displacement estimation of train 10 (41 km/h NB) using low-cost and commercial sensors. The figure shows that, although there are some inaccuracies, the overall behavior of the train is well captured by the low-cost sensors.

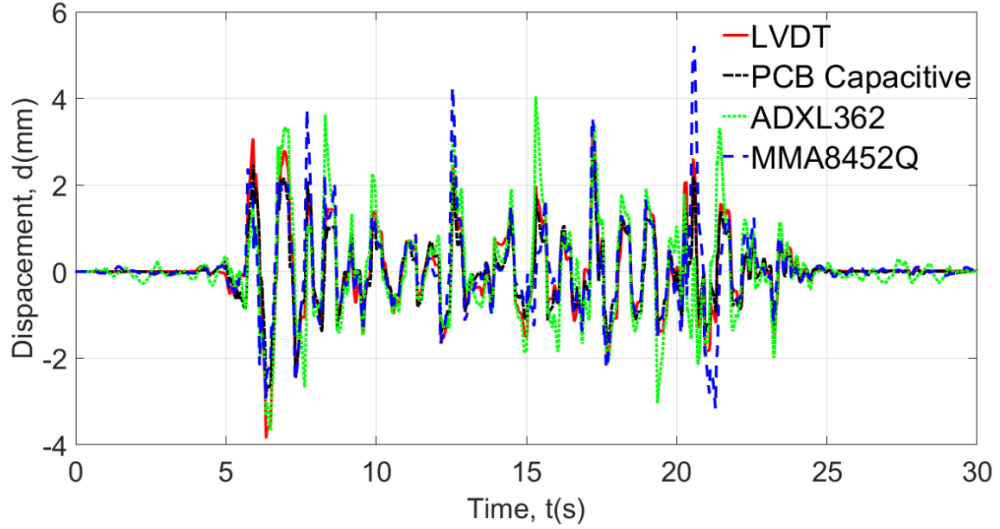


Fig. 4.14. Train displacement estimation for the 41 km/h NB case.

Fig. 4.15 shows that the  $E_3$  errors of the low-cost sensors (ADXL362 and MMA8452Q) are in all cases under 30 %.

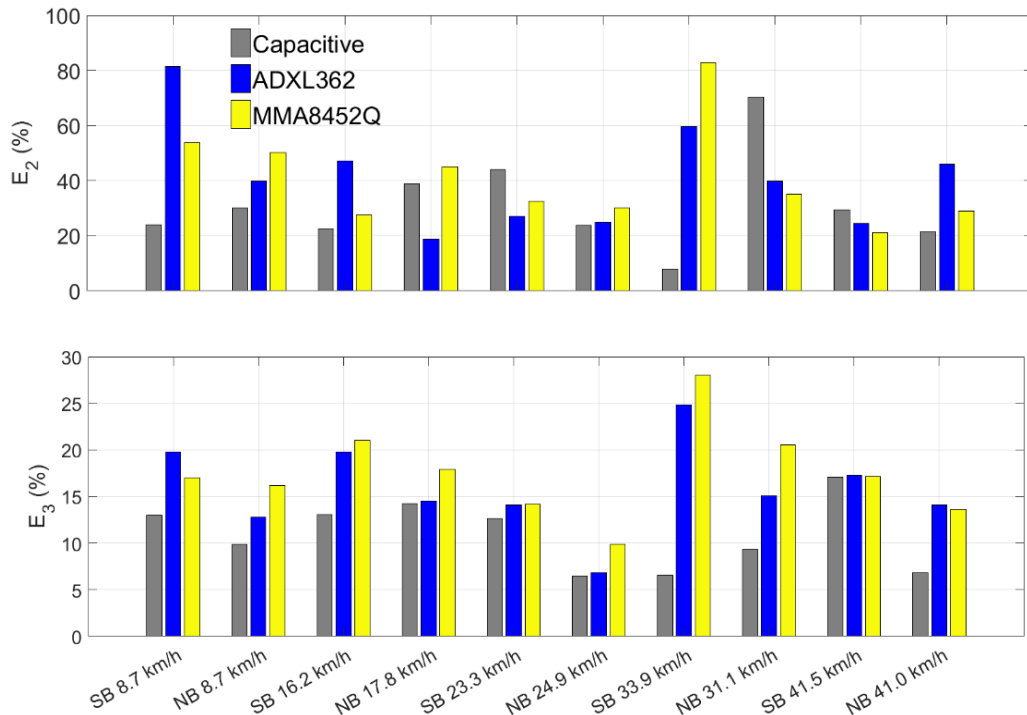


Fig. 4.15. Error values for Capacitive vs ADXL362 vs MMA8452Q for train tests.

The previously described low-cost accelerometers have embedded low-pass filters designed to improve the accuracy of the readings by eliminating the noise. However, these filters induce the underestimation of the signal, which might be the source of errors in the displacement estimations. In addition, these low-cost accelerometers have quantization errors that can be attributed to their low resolution with respect to the small variations of data that are being measured. In conclusion, the underestimation of the signal due to the embedded filters of the accelerometers and the quantization are contributing to the increase the error values obtained with the low-cost sensors. Still, in many comparisons, low-cost sensors were able to outperform commercial DAQ/sensor combinations.

Table 4.6. Train displacement estimation error.

Train (direction, speed)	$E_2(\%)$			$E_3(\%)$		
	Capacitive	ADXL362	MMA8452Q	Capacitive	ADXL362	MMA8452Q
SB 8.7 km/h	24.04	<b>81.51</b>	53.85	12.99	<b>19.79</b>	17.00
NB 8.7 km/h	30.03	39.85	<b>50.34</b>	9.86	12.79	<b>16.18</b>
SB 16.2 km/h	22.58	<b>47.20</b>	27.56	13.07	19.80	<b>21.04</b>
NB 17.8 km/h	38.78	18.74	<b>45.04</b>	14.24	14.52	<b>17.88</b>
SB 23.3 km/h	<b>44.20</b>	26.95	32.40	12.68	14.08	<b>14.14</b>
NB 24.9 km/h	23.86	24.92	<b>30.09</b>	6.51	6.85	<b>9.84</b>
SB 33.9 km/h	7.97	59.59	<b>82.91</b>	6.52	24.83	<b>28.03</b>
NB 31.1 km/h	<b>70.35</b>	39.87	35.15	9.35	15.06	<b>20.52</b>
SB 41.5 km/h	<b>29.50</b>	24.49	21.20	17.06	<b>17.32</b>	17.15
NB 41.0 km/h	21.37	<b>45.96</b>	28.91	6.84	<b>14.09</b>	13.65

Table 4.6 shows the error values of the reference-free bridge displacement estimation. The bold errors highlight the largest estimation error for each case.  $E_3$  error for low-cost estimations are always under 22 % with the exception of train 7 (SB 33.9 km/h). In that case, the errors are higher due to the harmonic roll that is taking place on the bridge. Railroads know that the harmonic roll is caused by the car-bridge interaction. Therefore, the errors are higher in both  $E_2$  and  $E_3$  performance indexes for train 7. In average, the low-cost estimation errors are 33 % for the all-peaks error ( $E_2$ ) and 13 % for the normalized root mean square error ( $E_3$ ). These results validate the use of low-cost sensors for reference-free displacement measurement of railroad bridges. The performance of the low-cost sensors are comparable to the results obtained by the Capacitive. The results of this research support the implementation of a monitoring technique with a much cheaper equipment, less implementation costs and more accessible sensors.

## **Chapter 5 Conclusions and further research**

### **5.1 Summary**

The efficient maintenance of railroad bridges is of crucial importance for the railroad network. Railroad bridges are aging and need to prioritize their maintenance and safety. However, most bridge inspections are mainly visual and therefore unable to assess the dynamic performance of the bridges under train live loading. Measuring bridge displacements under traffic can be used to assess the condition of railroad bridges. Traditional methods of structural health monitoring of railroad bridges difficult to implement due to the complexity and cost of the required equipment.

This study explores the ability of low-cost sensors in estimating bridge displacement. The performance of the low-cost sensors was compared to commercial accelerometers. A shake table was used to simulate the desired excitations and an LVDT collected the reference displacement data to use it as the reference signal. Three types of excitations were utilized to estimate their displacements: uniform sinusoidal waves, ground motion records and bridge vibrations measured on-site. The findings of this research indicate that low-cost sensors can estimate reference-free displacements of railroad bridges under dynamic loads. Results demonstrate that low-cost sensors can estimate displacements with 300 times less upfront investment than commercial accelerometers. In addition, comparisons have shown that low-cost sensors can be a successful alternative to the existing commercial sensors and can eventually be used to complement visual inspections. The accuracy of the estimation has an

average peak error of 40 % and a root mean square error of 15 % in the train displacement estimations. The estimation errors are comparable to those obtained by Moreu et al. (2015), which demonstrates the prospective benefits of using low-cost sensors for structural health monitoring of railroad bridges. There is still room for improvement regarding the use of low-cost sensors for SHM of railroad bridges but this research presents a successful first step towards a large scale implementation of low-cost sensors in the railroad industry. The method resulting from this study is potentially generalizable and applicable to any other vibrating structures such as highway bridges, wind turbines, or buildings located in seismically active regions.

In addition, this research also proposes a reference-free displacement estimation method based on the estimation of the pseudo-static and dynamic components of the displacement separately. A bridge model has been built and a shake table inputted the signals. The estimation has used the tilt angle of the bridge pier to obtain the pseudo-static component of the displacement and the deck accelerations the dynamic component estimation. Data filtering techniques transformed accelerations into displacements. Then, the estimated values are compared to the reference displacement and the error between them is calculated. This paper shows an average peak error of 10 % and a root mean square error average of 5 %. This method allows the estimation of the total displacement of the railroad bridge considering not only the dynamic component of the displacement as Moreu et al. (2015) estimated but also the pseudo-static displacement. The

findings of this research show that this method can be effectively used for structural health monitoring of railroad bridges.

## **5.2 Further research**

To further validate these methods, the next step would be to estimate bridge displacements on the field.

### **5.2.1 Wireless implementation**

One of the main potential improvements to the system would be to develop a wireless connection between the sensor and the computer that stores the data. In the case of the proposed low-cost sensor, that could be done by using the Arduino compatible wireless XBee modules. Such modules, can be easily hooked up to the Arduino board with minimum connection efforts. The transmitter would be connected to the sensing system and the receiver would be attached to the computer via USB connection. The open source software XCTU can be used to provide the wireless communication to communicate with the computer. Fig. 5.1 shows the configuration for the wireless connection.

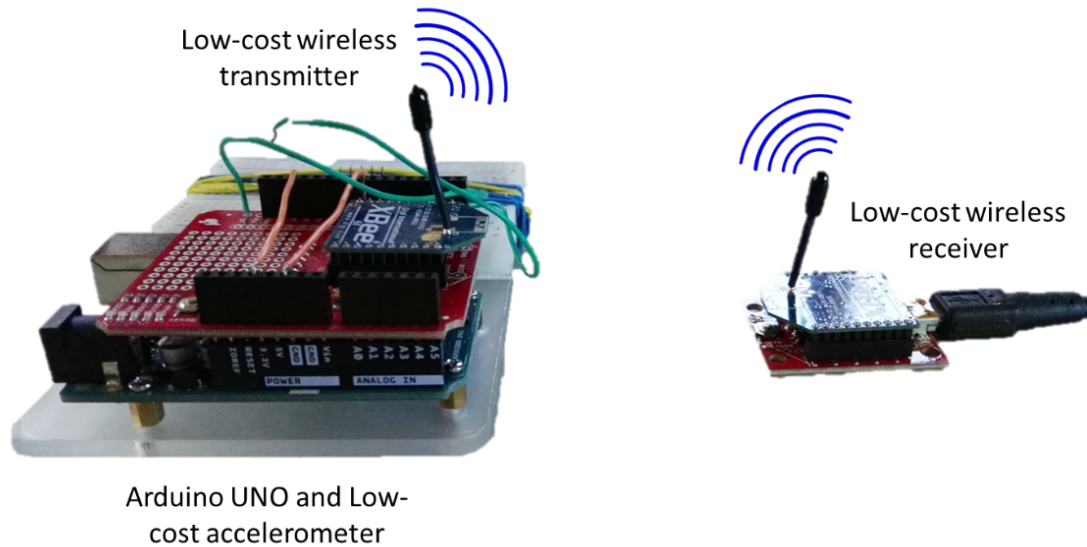


Fig. 5.1. Low-cost wireless connection configuration.

### 5.2.2 Power consumption

Due to the low-power consumption of the low-cost sensing systems, they can be powered with regular batteries or external DC power supplies. Another autonomous solution for powering the Arduino board is to use a Li-Po battery with a solar panel. That way, the battery is charged with the solar panel and can work without the need of external powering. It is also important to manage the power efficiently, especially when there are not any events occurring. In that case, putting the Arduino into low-consumption mode can help operate the sensor with less power. The sensor can always go back to the default mode when the measured values surpass the defined threshold.

### 5.2.3 Sensor casing and attachment

The defined low-cost sensor cannot be implemented for real life applications unless it is confined into a secure case that can protect it against the environmental



conditions such as wind, rain, snow, animals, etc. The design of a plastic case with a 3D printer is one of the options that could be explored. Due to the small dimensions and the cost of the 3D printing, the price of the case would be around ten dollars (depending on the material used). The sensor would then be attached with a magnet glued on the back of the case for steel bridges or with glues or resins if the sensor is meant to be permanent. Fig. 5.2 shows a tentative schematic representation of the final sensor.

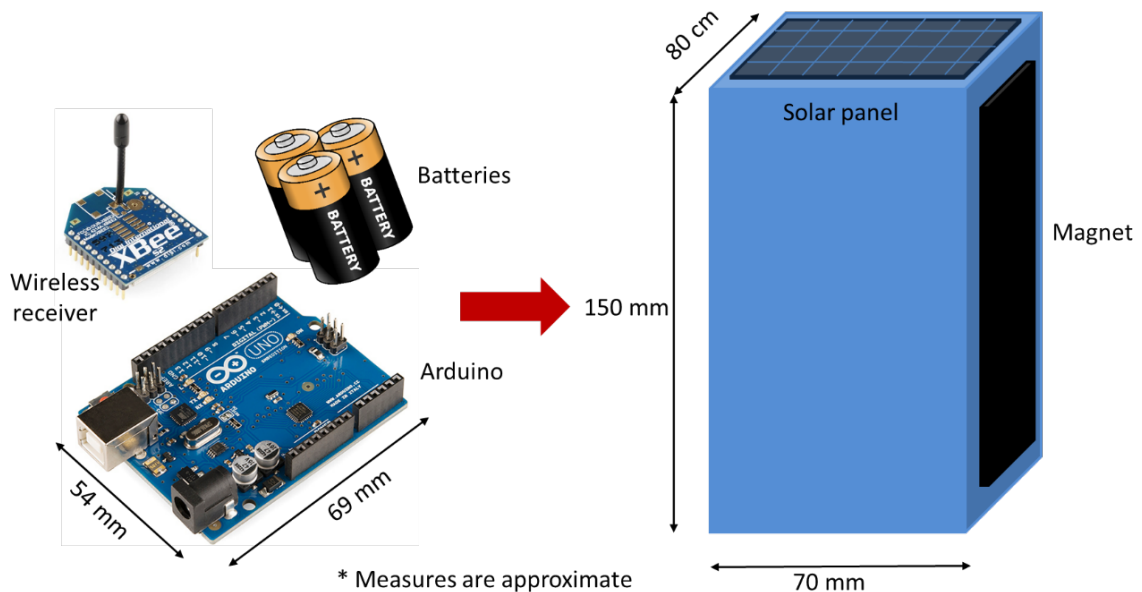


Fig. 5.2. Schematic configuration of final sensor.

This encasement would simplify the data acquisition greatly and would get rid of the cabling and the computer. One of the possibilities would be to power it with a solar panel feeding a rechargeable battery. In order for this system to work, the battery should have to be saved by setting a hibernation command to put the sensor to sleep. In addition, the sensor would be activated when the vibration surpassed a previously defined threshold.

#### 5.2.4 Low-cost tilt measurement

In the case of the tilt method, as it has been done with the dynamic displacement estimation, an Arduino-based low-cost sensing system could be implemented to estimate the pseudo-static displacement by measuring the angle of rotation of the bridge pier. To measure the angle with an Arduino, two possibilities could be explored: the first one would be to use one three-axis accelerometer and follow the method described in this paper calculating the arctangent from the two components of the acceleration of gravity. However, due to the reduction in accuracy compared to the commercial sensors, the errors would probably be higher than desired. The second option would be to use an inertial measurement unit (IMU) attached to the Arduino. An IMU consists of an accelerometer and a gyroscope. While the accelerometers measure the accelerations, the gyroscope measures the angular rate of change. There are plenty of ways of integrating both signals together, but one of the most simple and effective techniques is to use a complementary filter. This type of filter combines the two sensors taking their strengths and reducing the effect of their weaknesses. Accelerometers are very sensitive to noise, but they tend to capture the overall trend of the curve with decent accuracy. On the other hand, gyroscopes are very precise and not susceptible to noise but tend to drift over time due to the iterative addition of unknown constants of integration. With this filter, the angle of rotation can be estimated with acceptable accuracy. Equation 5.1 defines the relation between the two IMU sensors used by the complementary filter:

$$angle(t_i) = k_1 \cdot (angle(t_{i-1}) + w_{gyro} \cdot dt) + k_2 \cdot (a_{accel}) \quad (5.1)$$

where  $angle(t_i)$  and  $angle(t_{i-1})$  are the values of the angle in the current and the previous step respectively,  $k_1$  and  $k_2$  are two user-defined constants that control the amount of data that is taken from each sensor. The sum of them has to be 1 in order for the filter to be tuned properly. The angular velocity measured by the gyroscope is given by  $w_{gyro}$ , which is multiplied by the time increment  $dt$ . Finally,  $a_{accel}$  is the acceleration value measured by the accelerometer.

Fig. 5.3 shows the set-up for the low-cost tilt measurement estimation. In the figure, the Arduinos are placed on a plate attached to the pile bent model to capture the angular changes. Since the proposed low-cost accelerometers are tri-axial, only one of them would be necessary.

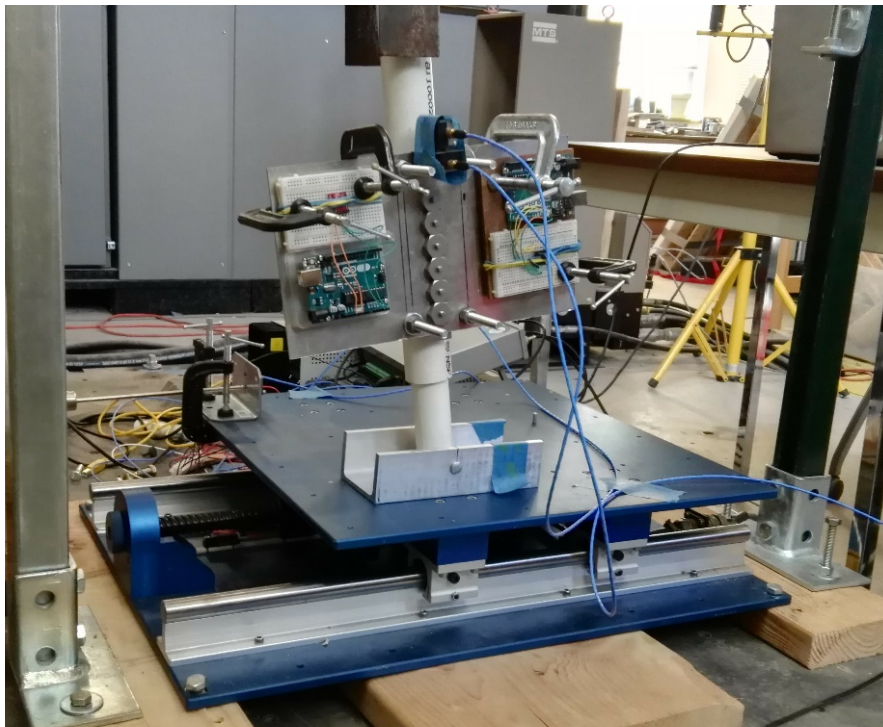


Fig. 5.3. Low-cost tilt measurement estimation set-up.

## **5.4 Limitations**

This research has some limitations that have to be acknowledged. The first one is that the results obtained in chapter 3 (inclination angle displacement estimation) are biased due to the use of the same set of data for building the filter and for testing it. Therefore, different bridge excitations should be tested to obtain a more complete bridge parameter definition. Another fact that has to be taken into account is that all the experimentation described in this research has been conducted in a laboratory and therefore, in unrealistic conditions. If these methods were to be implemented on the field, there are some aspects ignored in this paper that would have to be taken into consideration such as the thermal drift of the sensors, the powering of the sensing systems or their attachment to the bridge. Finally, a more realistic model would have to be built to take further steps in the angle displacement estimation. The model used in this research had a smaller movement to pier height ratio, resulting in larger angles and therefore larger measured accelerations.

## **5.3 Applications**

The proposed methods can be implemented in the field with limited training and basic technical knowledge of sensing technologies. In addition, the low-cost and the availability of the proposed sensing technology allows easy replacement and a more complete analysis of the bridges by placing larger number of sensors. Railroad industry can benefit from the implementation of such technology and it

would make it possible to manage the network more efficiently and successfully prioritize the maintenance of bridges.

## **5.5 Publications related to this MS thesis document**

The results of this research have been presented at international technical conferences and is currently under review by international technical journals in smart structures and structural health monitoring, as noted below:

- Gomez, J. A., Ozdagli, A. I., Moreu, F. (2017). Total Reference-Free Displacements for Condition Assessment of Timber Railroad Bridges Using Tilt. Smart Structures and Systems. <http://technopress.kaist.ac.kr/?journal=sss> (Chapter 3 in this MS thesis)
- Ozdagli, A. I., Moreu, F., Gomez, J. A., Garp, P., Vemuganti, S. (2016). Data Fusion of Accelerometers with Inclinometers for Reference-free High Fidelity Displacement Estimation. European Workshop on Structural Health Monitoring. <http://www.ndt.net/events/EWSHM2016/app/content/index.php?eventID=34> (Chapter 3 in this MS thesis)
- Gomez, J. A., Ozdagli, A. I., Moreu, F. (2016). Application of Low-Cost Sensors for Estimation of Reference-Free Displacements Under Dynamic Loading for Railroad Bridges Safety. Conference on Smart Materials, Adaptive Structures and Intelligent Systems. <https://www.asme.org/events/smasis> (Chapter 4 in this MS thesis)

- Gomez, J. A., Ozdagli, A. I., Moreu, F. (2017). Reference-Free Dynamic Displacements of Railroad Bridges Using Low-Cost Sensors. Journal of Intelligent Materials Systems and Structures. <https://us.sagepub.com/en-us/nam/journal/journal-intelligent-material-systems-and-structures> (Chapter 4 in this MS thesis)

## References

- Agdas, D., Rice, J. A., Martinez, J. R., & Lasa, I. R. (2015). Comparison of visual inspection and structural-health monitoring as bridge condition assessment methods. *Journal of Performance of Constructed Facilities*, 30(3), 04015049.
- Analog Devices. (2015a) "ADXL345 Data Sheet". Retrieved from <http://www.analog.com/media/en/technical-documentation/data-sheets/ADXL345.pdf>.
- Analog Devices. (2015b) "ADXL362 Data Sheet". Retrieved from <http://www.analog.com/media/en/technical-documentation/data-sheets/ADXL362.pdf>.
- Andò, B., Baglio, S., & Pistorio, A. (2014). A low cost multi-sensor strategy for early warning in structural monitoring exploiting a wavelet multiresolution paradigm. *Procedia Engineering*, 87, 1282-1285.
- Arduino (2015). Retrieved from: "<https://www.arduino.cc/>".
- AREMA (2003); Practical Guide to Railway Engineering.
- Association of American Railroads (AAR). (2013) "AAR 2013 Total Annual Spending Data". Retrieved from [https://www.aar.org/Fact%20Sheets/Safety/2013-AAR\\_spending-graphic-fact-sheet.pdf](https://www.aar.org/Fact%20Sheets/Safety/2013-AAR_spending-graphic-fact-sheet.pdf)
- Association of American Railroads (AAR). (2013) "Our Network, Economic and public benefits". Retrieved from <https://www.aar.org/todays-railroads/our-network#maintain>.
- Association of American Railroads (AAR). (2015) "AAR Outlook 2015". Retrieved from <https://www.aar.org/Documents/Outlook%202015/2015OutlookReport.pdf>
- Association of American Railroads (AAR). (2016) "Bridging America: Maintaining Our Rail Bridges, Freight Rail Works.". Retrieved from <http://archive.freightrailworks.org/videos/bridging-america/>.
- Balageas, D., Fritzen, C. P., & Güemes, A. (2006). *Structural health monitoring* (Vol. 493). London, UK: ISTE.
- Barke, D., & Chiu, W. K. (2005). Structural health monitoring in the railway industry: a review. *Structural Health Monitoring*, 4(1), 81-93.
- Boore, D. M. (2003). "Analog-to-digital conversion as a source of drifts in displacements derived from digital recordings of ground acceleration." *Bull.Seism.Soc.Am.*,93(5),2017–2024.
- Cambridge Systematics, Inc. (2007) "National Rail Freight Infrastructure Capacity and Investment Study."
- Chougule, P., Kirkegaard, P. H., & Nielsen, S. R. (2010). Low cost wireless sensor network for structural health monitoring. In *Scandinavian vibration forum: skandinaviska vibrationsforenigen (SVIB)*, Linköping, Sweden (pp. 1-4).
- Embedded Computing Design. (2016). Retrieved from: "<http://embedded-computing.com/guest-blogs/arduino-development-boards-the-uno/>"

- Fanning, P. J., Sobczak, L., Boothby, T. E., & Salomoni, V. (2005). Load testing and model simulations for a stone arch bridge. *Bridge Structures, Assessment, Design and Construction*, 1(4), 367-378.
- Farrar, C. R., Baker, W. E., Bell, T. M., Cone, K. M., Darling, T. W., Duffey, T. A., ... & Migliori, A. (1994). Dynamic characterization and damage detection in the I-40 bridge over the Rio Grande (No. LA--12767-MS). Los Alamos National Lab., NM (United States).
- Federal Railroad Administration (FRA). (2010). "Bridge Safety Standards; Final Rule". Retrieved from <http://www.fra.dot.gov/eLib/details/L03212>.
- Federal Railroad Administration (FRA). (2015). "Freight Railroads Background" Office of Policy, Office of Rail Policy and Development, Federal Railroad Administration. Retrieved from <https://www.fra.dot.gov/eLib/Details/L03011>.
- GeoMetrx, (2013). "High Speed Rail: A Vision for the Future". Retrieved from: "geomtrx.com".
- Gindy, M., Vaccaro, R., Nassif, H., and Velde, J. (2008). "A state-space approach for deriving bridge displacement from acceleration." *Comput.-Aided Civ. Infrastruct. Eng.*, 23(4), 281–290.
- Hoag, A., Hoult, N., Take, A., Moreu, F., Le, H., Tolikonda, V. (2017). "Measuring displacements of a railroad bridge using DIC and accelerometers". *Smart Structures and Systems*. 19(2), 225-236.
- Hou, X., Yang, X., & Huang, Q. (2005). Using inclinometers to measure bridge deflection. *Journal of Bridge Engineering*, 10(5), 564-569.
- Hussain, S. M. A., Garg, V. K., & Singh, S. P. (1980). Harmonic roll response of a railroad freight car. *Journal of Engineering for Industry*, 102(3), 282-288.
- Kim, S., Pakzad, S., Culler, D., Demmel, J., Fenves, G., Glaser, S., & Turon, M. (2007). Health monitoring of civil infrastructures using wireless sensor networks. In 2007 6th International Symposium on Information Processing in Sensor Networks (pp. 254-263). IEEE.
- Lee, H. S., Hong, Y. H., & Park, H. W. (2010). Design of an FIR filter for the displacement reconstruction using measured acceleration in low-frequency dominant structures. *International Journal for Numerical Methods in Engineering*, 82(4), 403-434.
- M+P International (2015). "Vibpilot description" Retrieved from [http://www.mpihome.com/files/pdf/vibpilot\\_us.pdf](http://www.mpihome.com/files/pdf/vibpilot_us.pdf)
- MATLAB and Statistics Toolbox (2015). [Computer Software]. The MathWorks, Inc., Natick, Massachusetts, United States.
- Min, J. H., Gelo, N. J., & Jo, H. (2016). Real-time image processing for non-contact monitoring of dynamic displacements using smartphone technologies. In SPIE Smart Structures and Materials+ Nondestructive Evaluation and Health Monitoring (pp. 98031B-98031B). International Society for Optics and Photonics.
- Moreu, F., Jo, H., Li, J., Kim, R. E., Cho, S., Kimmle, A., ... & LaFave, J. M. (2014). Dynamic assessment of timber railroad bridges using displacements. *Journal of Bridge Engineering*, 20(10), 04014114.



- Moreu, F., & LaFave, J. M. (2011). Survey of Current Research Topics--Railroad Bridges and Structural Engineering. *Railway Track and Structures*, 107(9).
- Moreu, F., & LaFave, J. M. (2012). Current research topics: Railroad bridges and structural engineering. Newmark Structural Engineering Laboratory. University of Illinois at Urbana-Champaign..
- Moreu, F., & Nagayama, T. (2008). Use of wireless sensors for timber trestle railroad bridges health monitoring assessment. In Proc., 2008 Structures Congress.
- Moreu-Alonso, F. (2015). Framework for risk-based management and safety of railroad bridge infrastructure using wireless smart sensors (WSS) (Doctoral dissertation, University of Illinois at Urbana-Champaign).
- Murray, C. (2013). Dynamic Monitoring of Rail and Bridge Displacements using Digital Image Correlation.
- Nassif, H. H., Gindy, M., & Davis, J. (2005). Comparison of laser Doppler vibrometer with contact sensors for monitoring bridge deflection and vibration. *ND T & E International*, 38(3), 213-218.
- N. E. Bridge Contractors Inc. (2016). Retrieved from: "<http://www.bridgeriggers.com/hi-rail-services/hi-rail-under-bridge-units>"
- Nickitopoulou, A., Protopsalti, K., & Stiros, S. (2006). Monitoring dynamic and quasi-static deformations of large flexible engineering structures with GPS: accuracy, limitations and promises. *Engineering Structures*, 28(10), 1471-1482.
- NXP Semiconductors. (2015) "MMA8452Q Data Sheet". Retrieved from [http://cache.nxp.com/files/sensors/doc/data\\_sheet/MMA8452Q.pdf](http://cache.nxp.com/files/sensors/doc/data_sheet/MMA8452Q.pdf).
- Ojeda, L., & Borenstein, J. (2007). Non-GPS navigation for security personnel and first responders. *Journal of Navigation*, 60(03), 391-407.
- Park, J. W., Sim, S. H., & Jung, H. J. (2013). Development of a wireless displacement measurement system using acceleration responses. *Sensors*, 13(7), 8377-8392.
- PCB Piezotronics. (2015). "3711E1110G Product Manual". Retrieved from <http://www.pcb.com/Products.aspx?m=3711E1110G>.
- Peairs, D. M., Park, G., & Inman, D. J. (2004). Improving accessibility of the impedance-based structural health monitoring method. *Journal of Intelligent Material Systems and Structures*, 15(2), 129-139.
- Perez-Pena, R. (1996). "Rail Accident Stirs Debate about Sensors." *The New York Times*, November 29.
- Psimoulis, P. A., & Stiros, S. C. (2013). Measuring deflections of a short-span railway bridge using a robotic total station. *Journal of Bridge Engineering*, 18(2), 182-185.
- Quanser. (2016) "Quanser shake table Data Sheet". Retrieved from [http://www.quanser.com/Products/Docs/3985/Shake\\_Tables\\_and\\_Smart\\_Structures\\_System\\_Specifications\\_v1.6.pdf](http://www.quanser.com/Products/Docs/3985/Shake_Tables_and_Smart_Structures_System_Specifications_v1.6.pdf).
- RDP Electrosense (2016) "DCTH Series DC to DC LVDT Displacement Transducer". Retrieved from <http://www.rdpe.com/ex/dcth.pdf>

- Roumeliotis, S. I., Johnson, A. E., & Montgomery, J. F. (2002). Augmenting inertial navigation with image-based motion estimation. In *Robotics and Automation, 2002. Proceedings. ICRA'02. IEEE International Conference on* (Vol. 4, pp. 4326-4333). IEEE.
- Sabatini, A. M. (2006). Quaternion-based extended Kalman filter for determining orientation by inertial and magnetic sensing. *IEEE Transactions on Biomedical Engineering*, 53(7), 1346-1356.
- SMILab (2017). "Facilities" Retrieved from <http://smilab.unm.edu/index.php/home-2/facilities-2/>
- Spencer Jr, B. F., Moreu, F., & Kim, R. E. (2015). Campaign Monitoring of Railroad Bridges in High-Speed Rail Shared Corridors using Wireless Smart Sensors. Newmark Structural Engineering Laboratory. University of Illinois at Urbana-Champaign.
- Stephen, G. A., Brownjohn, J. M. W., & Taylor, C. A. (1993). Measurements of static and dynamic displacement from visual monitoring of the Humber Bridge. *Engineering Structures*, 15(3), 197-208.
- Sundaram, B. A., Parivallal, S., Kesavan, K., Ahmed, A. K. F., Ravisankar, K., Ramanjaneyulu, K., & Iyer, N. R. (2015). Condition assessment of a prestressed concrete girder and slab bridge for increased axle loadings. *Journal of Scientific & Industrial Research*, 74, 634-640.
- Systematics, C. (2007). National rail freight infrastructure capacity and investment study. Cambridge Systematics, Cambridge.
- Unsworth, J. F. (2010). Design of modern steel railway bridges. CRC Press
- Uppal, A. S., Rizkalla, S. H., & Pinkney, R. B. (1990). Response of timber bridges under train loading. *Canadian Journal Of Civil Engineering*, 17(6), 940-951. doi:10.1139/l90-106
- Villemure, I., Ventura, C. E., & Sexsmith, R. G. (1996). Impact and Ambient Vibration Testing To Assess Structural Damage In Reinforced Concrete Frames. In *PROCEEDINGS-SPIE THE INTERNATIONAL SOCIETY FOR OPTICAL ENGINEERING* (pp. 1178-1184). SPIE INTERNATIONAL SOCIETY FOR OPTICAL.
- Watson, C., Watson, T., & Coleman, R. (2007). Structural monitoring of cable-stayed bridge: analysis of GPS versus modeled deflections. *Journal of Surveying Engineering*, 133(1), 23-28.
- Yang, J., Li, J.B., and Lin, G. (2005). "A simple approach to integration of acceleration data for dynamic soil-structure interaction analysis". 2012 ASCE Structures Congress, Proceedings. ASCE-SEI, March.
- Yu, Y., Zhao, X., & Ou, J. (2012). A new idea: Mobile structural health monitoring using Smart phones. In *Intelligent Control and Information Processing (ICICIP), 2012 Third International Conference on* (pp. 714-716). IEEE.
- Yu, Y., Liu, H., Li, D., Mao, X., & Ou, J. (2013). BRIDGE DEFLECTION MEASUREMENT USING WIRELESS MEMS INCLINATION SENSOR SYSTEMS. *International Journal on Smart Sensing & Intelligent Systems*, 6(1).

- Zhang, Z., & Aktan, A. E. (1995). The damage indices for the constructed facilities. In PROCEEDINGS-SPIE THE INTERNATIONAL SOCIETY FOR OPTICAL ENGINEERING (pp. 1520-1520). SPIE INTERNATIONAL SOCIETY FOR OPTICAL.
- Zhang, W., Sun, L. M., & Sun, S. W. (2016). Bridge-Deflection Estimation through Inclinometer Data Considering Structural Damages. Journal of Bridge Engineering, 04016117.